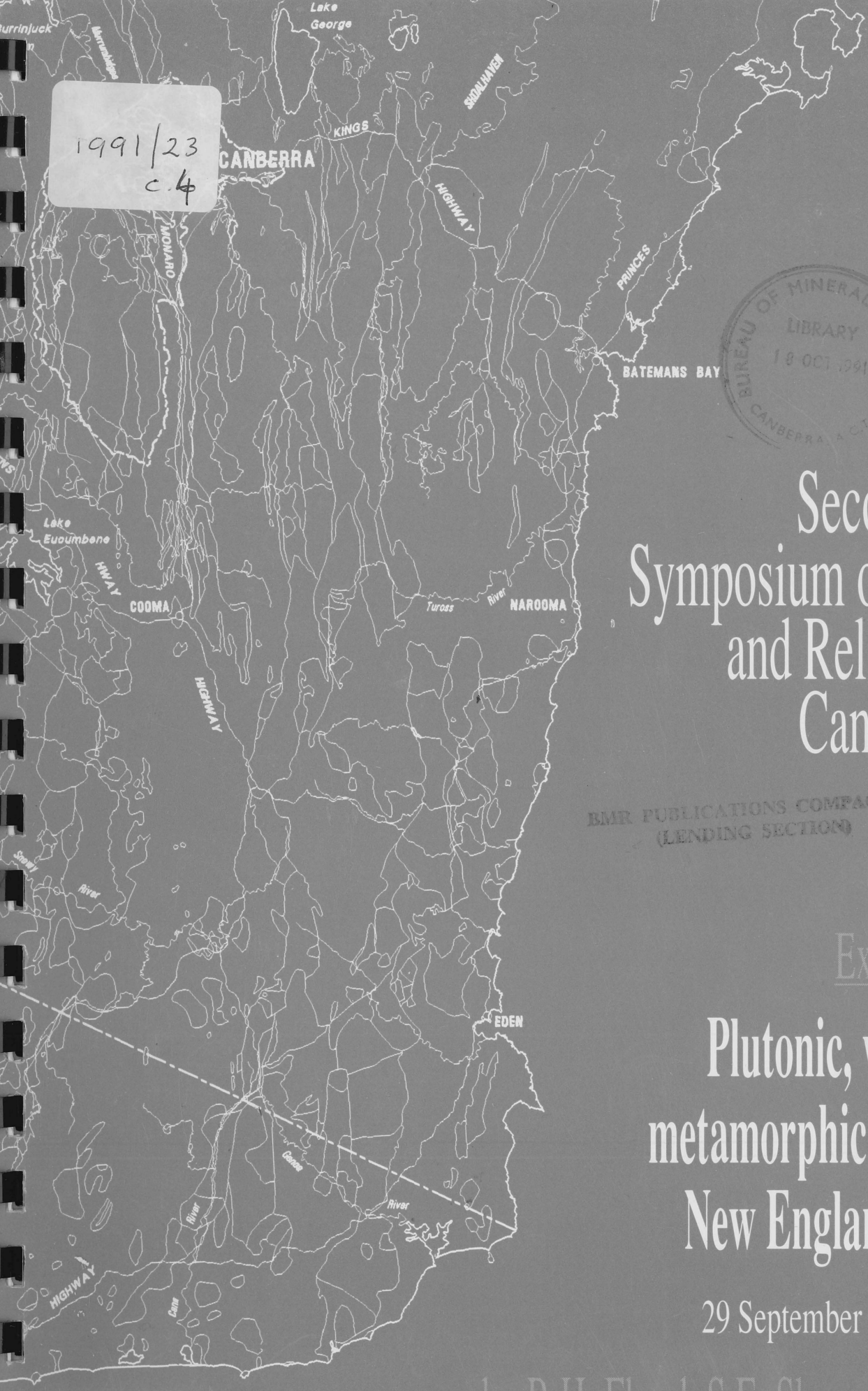

BMR
GEOLOGY AND
GEOPHYSICS
AUSTRALIA

Second Hutton Symposium on Granites and Related Rocks Canberra 1991

Excursion Guide

Plutonic, volcanic and metamorphic rocks of the New England Batholith

29 September - 4 October 1991

by R.H. Flood, S.E. Shaw & T.R. Farrell

1991/23
c.4

Record 1991/23

Second Hutton Symposium on Granites and Related Rocks

Canberra 1991

Excursion Guide

Plutonic, volcanic and metamorphic rocks of the New England Batholith

29 September - 4 October 1991

by

R.H. Flood, S.E. Shaw & T.R. Farrell

Bureau of Mineral Resources, Geology and Geophysics

Record 1991/23

ISSN 0811-062 X

ISBN 0 642 16651 X

HUTTON CONFERENCE 1991

NEW ENGLAND BATHOLITH EXCURSION

R.H. FLOOD, S.E. SHAW AND T. FARRELL

SUNDAY TRAVEL FROM CANBERRA TO BENDEMEER

MONDAY

Stops.
1-1 Western margin of the Bendemeer pluton where it is most mafic.
1-2 Eastern contact of the Bendemeer pluton where it is most felsic.
1-3 Contact metamorphic rocks between the Bendemeer and Walcha Road plutons.
1-4 Typical porphyritic Walcha Road Adamellite 0.5 km west of Congi Creek.
1-5 Eastern contact of the pluton at Surveyors Creek.
1-6 Pyroxene phenocryst locality.
1-7 Enclave-rich locality on the Macdonald River (ES7)
1-8 Railway crossing, Oxley Higway just east of Woolbrook
1-9 Congi Creek leucocratic central zone 3 km east of Congi Creek.
1-10 Enclave-rich margin at Rimbanda Station.
1-11 Looanga pluton and its enclaves, road cut, New England Highway.

THE WALCHA ROAD PLUTON - A ZONED, RESTITE-POOR PLUTON

The important inferences from a study of this pluton include: (a) Sidewall crystallisation and variation in water activity have produced the compositional and microstructural zonation: (b) Euhedral pyroxene megacrysts present in the marginal facies of the pluton exhibit oscillatorty zoning and are of igneous origin: (c) Reaction of these pyroxenes with the magma produce some and perhaps all of the mafic clots that are inferred by some authors to be restite: (d) In several localities around the pluton are small monzodiorite stocks that are so fine-grained that they can hide little restite and as such indicate the presence of intermediate K-rich restite-poor magmas: (d) The inferred subsurface shape of the pluton indicates that the outer more-mafic zones of the pluton account for a much larger volume-proportion of the pluton than the leucocratic central zones: (e) The enclaves vary from porphyritic-microgranodiorites, not

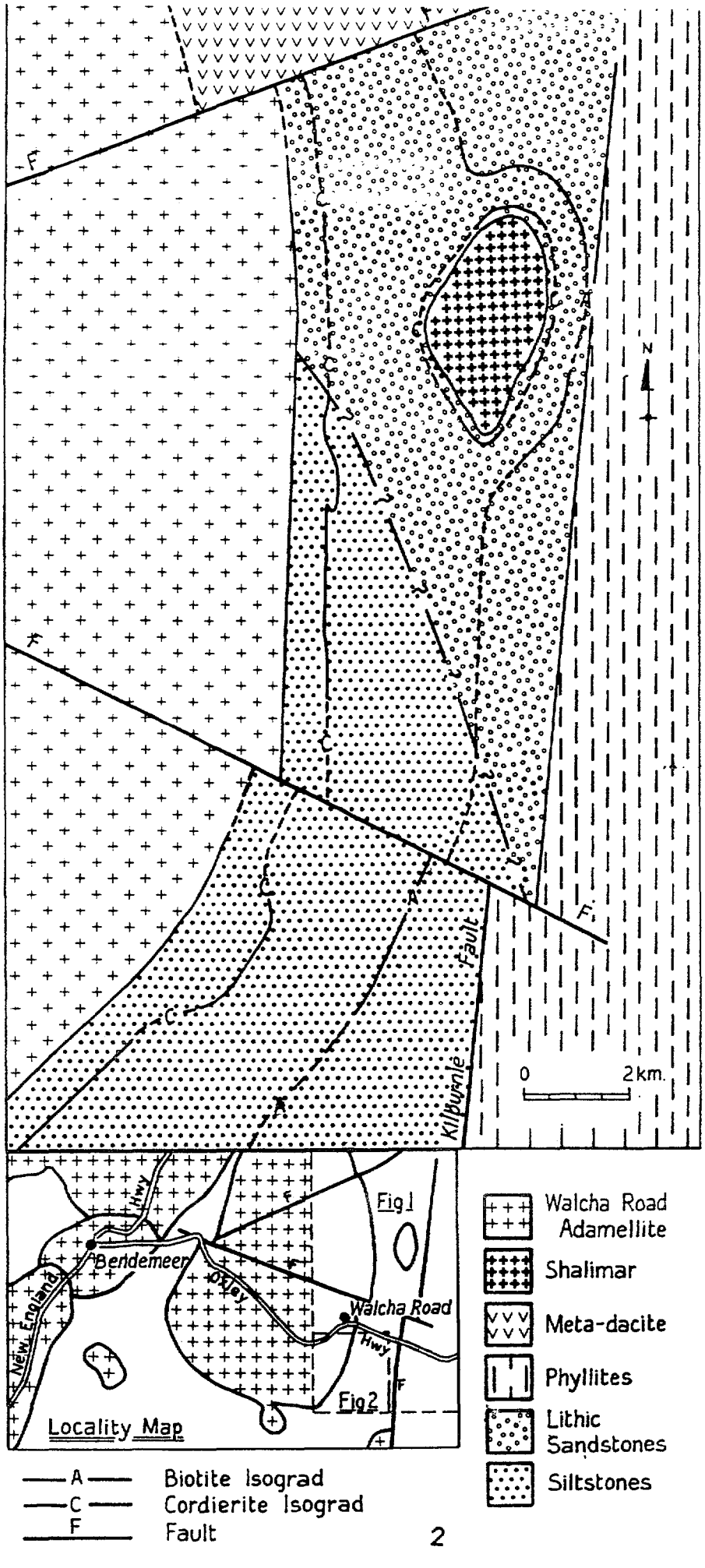

Map redrawn from Teale 1974 showing the wide thermal aureole around the Walch Road pluton which overlaps the aureole of the much smaller Shalimar pluton.

Fig 1

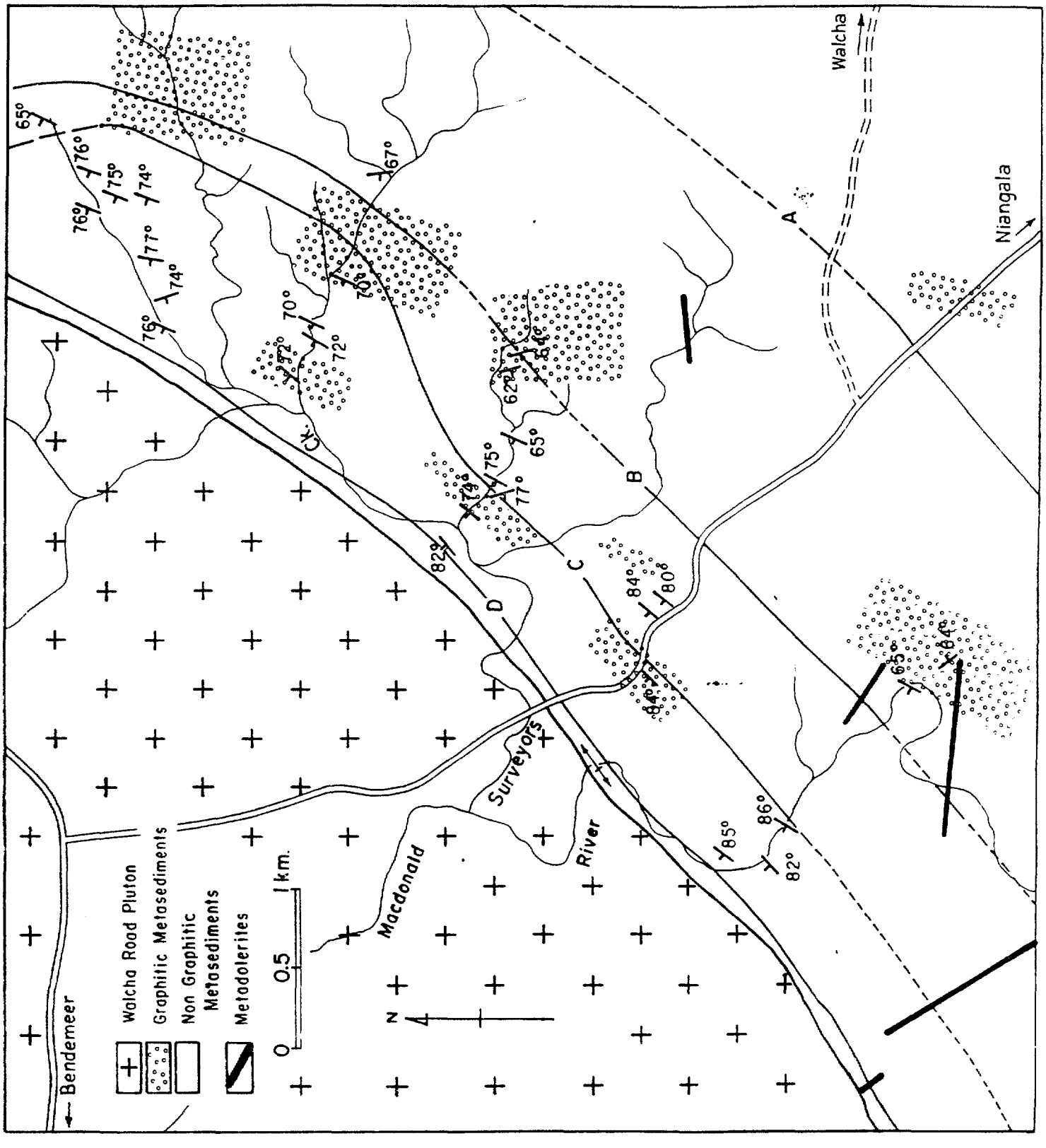

Fig 2 Detail of the contact metamorphic zonation of the contact schists along the south-east margin of the Walcha Road pluton (from Teale, 1974). A-biotite isograd, B-andalusite isograd, C-cordierite isograd and D- cordierite - K-feldspar isograd.

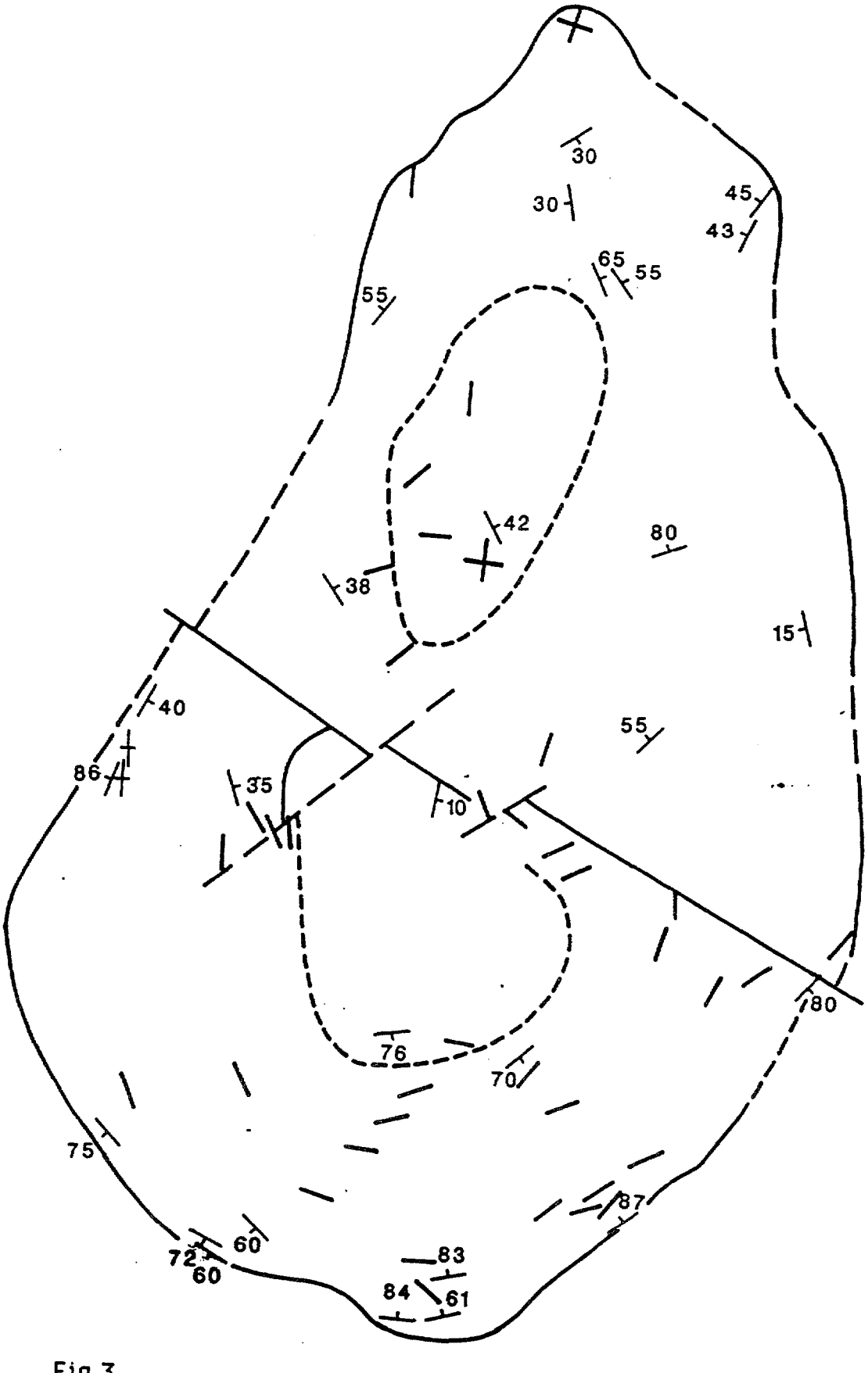

Fig 3

Structural data for the Walcha Road pluton. Foliation measurements obtained by measuring the orientation of the long axes of 200 K-feldspar phenocrysts. A sample of only ten or twenty microgranitoid enclaves gives similar results.

significantly different from the pluton, to hornblende syenite compositions. Some K-feldspar in the syenites could be the result of reaction of the enclave with the magma but most of the K-feldspar forms large poikilitic grains that include the other minerals of the enclave in the same way that quartz grains do in many of the more silica-rich enclaves in this and other plutons. To explain the origin of these enclaves by the pressure-quench model would require that they formed from a range of magma compositions from monzonite to adamellite: (f) Chemical data from the pluton show a silica gap between 64 and 67 percent. We suggest the gap separates "cumulate" marginal rocks from rocks that more closely represent the magma from which they crystallized: (g) The microgranitoid enclaves (MGE) occur mostly in rocks slightly more silica-rich than the "silica gap".

The Walcha Road pluton has a 3 km wide aureole of hornfelses above the biotite isograd. The aureole along the eastern contact has been mapped by Teale (1974) and his zonation is shown in Figs 1 and 2. Teale noted that the highest grade contact rocks are schists some of which have a fine metamorphic compositional layering. He also observed that the metamorphic foliation deflects around the cordierite porphyroblasts in a way that implies a degree of contact-normal shortening after growth of cordierite.

The Walcha Road pluton of southern New England is 40 km long, 20 km wide and elliptical in outline. Botite/bulk rock ages for the pluton and small quartz monzodiorite stocks along the southern and western margin give Late Permian ages of approximately 247 Ma and initial 87Sr/86Sr ratios of 0.7046.

A foliation defined by the preferred orientation of the major axes of both feldspar and, where present, microgranitoid enclaves is generally margin parallel (Fig 3). Around the southern margin of the pluton, dips are steeply inward suggesting a cone shape for that part of the pluton. A lineation present in samples near the margin is consistently down-dip. Modal, chemical and microstructural variations within the pluton define a concentric zoning pattern (Fig 4). The pluton is zoned from a marginal quartz monzonite (colour index = 35) with hornblende in excess of biotite, to a hornblende-free biotite-adamellite (colour index = 6) in the centre. The discontinuous marginal quartz-monzonite, which contains white K-feldspar, is even-grained and grades over a few tens of metres into a porphyritic mafic adamellite in which the K-feldspar megacrysts are pink and up to 10 mm in length and

A Chemical variation of Walcha Road pluton along section A - B B

	FS801	FS803	FS849	FS848	FS809	FS840	FS810	FS811	FS815	FS816	FS822	FS824	FS825	FS833	FS828
SiO2	67.51	69.18	68.36	69.78	69.29	69.78	71.37	71.45	71.23	70.72	69.36	68.02	66.97	63.71	63.76
TiO2	0.56	0.50	0.49	0.37	0.45	0.38	0.29	0.29	0.31	0.39	0.39	0.51	0.56	0.69	0.78
Al2O3	14.93	14.18	14.18	14.00	14.65	14.24	14.39	14.65	14.42	14.46	14.45	14.66	14.87	14.66	14.50
Fe2O3	1.09	1.09	1.22	0.98	0.98	0.72	0.58	0.80	0.78	1.10	1.07	1.38	1.42	1.65	1.25
FeO	2.18	1.90	1.70	1.26	1.69	1.52	1.25	1.28	1.13	1.26	1.25	1.59	1.87	2.52	3.29
MnO	0.08	0.07	0.07	0.06	0.07	0.06	0.05	0.05	0.05	0.06	0.06	0.07	0.08	0.09	0.09
MgO	2.03	1.74	2.09	1.49	1.68	1.45	0.79	0.78	0.85	1.28	1.42	1.82	2.10	3.20	3.46
CaO	3.22	2.99	2.94	2.49	2.86	2.28	2.35	2.33	2.35	2.70	2.84	2.98	3.21	3.93	3.98
Na2O	3.56	3.59	3.70	3.59	3.55	3.64	3.85	4.01	3.81	4.14	3.86	3.65	3.66	3.38	3.38
K2O	4.27	3.94	3.92	4.12	4.42	4.51	3.80	3.45	4.00	3.64	3.78	4.28	4.04	4.48	4.31
P2O5	0.23	0.20	0.17	0.11	0.19	0.12	0.05	0.07	0.08	0.12	0.12	0.16	0.20	0.31	0.35
H2O+	0.87	0.82	0.90	1.00	0.72	0.66	0.65	0.87	0.78	0.59	0.80	0.77	0.61	0.74	0.71
H2O-	0.06	0.07	0.13	0.11	0.09	0.10	0.16	0.04	0.05	0.00	0.06	0.04	0.02	0.07	0.00
CO2	0.03	0.03	0.00	0.00	0.04	0.07	0.09	0.12	0.04	0.27	0.05	0.02	0.06	0.11	0.09
TOTAL	100.62	100.30	99.87	99.36	100.68	99.53	99.67	100.19	99.88	100.73	99.51	99.95	99.67	99.54	99.95
Ba	720	500	556	486	594	647	619	537	649	487	539	792	713	1123	1144
Cr	68	54	50	36	42	33	10	7	11	27	35	48	62	98	124
Cu	16	11	6	5	12	17	6	3	6	11	5	8	11	18	15
Ga	20	19	19	19	19	20	17	21	18	18	19	21	20	21	21
Nb	14	21	0	0	8	9	12	7	7	11	10	9	17	8	5
Ni	17	15	12	13	11	11	6	6	8	12	11	16	17	22	29
Pb	32	34	28	31	32	35	23	23	29	29	28	28	29	36	33
Rb	191	223	210	205	195	225	167	158	188	180	180	195	207	195	200
Sr	476	397	408	360	403	374	400	417	373	409	416	442	442	624	618
Th	36	35	32	29	35	32	30	24	31	29	27	28	36	44	34
U	7	13	10	12	10	13	13	13	8	9	8	10	10	9	9
V	73	60	60	44	51	44	23	23	27	40	46	59	71	89	111
Y	20	20	16	13	18	15	16	17	18	16	16	17	19	25	24
Zn	52	46	47	36	43	39	36	35	38	44	40	47	53	58	65
Zr	163	157	138	109	136	116	124	116	135	119	120	141	158	211	212

Table 1

Chemical variation of associated monzodiorite stock

	MG2	MG14	MG15	MG22	RF6
SiO2	59.37	61.01	61.09	61.53	63.31
TiO2	1.00	0.91	0.85	0.97	0.88
Al2O3	15.15	15.81	15.34	14.68	16.43
Fe2O3	1.29	1.60	1.42	1.41	1.19
FeO	4.93	4.56	4.26	4.75	4.38
MnO	0.13	0.12	0.10	0.11	0.12
MgO	4.55	2.66	4.32	4.63	3.09
CaO	6.08	5.01	5.72	5.55	5.50
Na2O	2.65	3.19	3.00	2.19	2.60
K2O	3.80	4.05	3.25	2.89	3.01
P2O5	0.34	0.42	0.29	1.31	0.23
H2O+	0.25	0.39	0.49	0.61	0.25
H2O-	0.05	0.27	0.12	0.19	0.05
TOTAL	99.59	100.00	100.25	100.82	101.04
Ba	1053	1157	825	625	1194
Ga	16	19	18	17	22
Pb	30	40	27	25	31
Rb	171	182	262	150	168
Sr	504	513	425	413	433
Th	18	21	14	24	19
U	5	6	4	6	6
Y	26	26	24	22	23
Zr	242	259	191	232	207

Chemical variation of enclaves

	FS8X	FS1X	FS5X	FS6X	WR8XA	WR1X	NEB64X
SiO2	56.78	58.60	59.29	63.63	65.12	66.06	66.50
TiO2	0.90	1.07	0.64	0.73	0.72	0.71	0.62
Al2O3	13.21	15.20	11.77	14.93	15.39	15.48	15.30
Fe2O3	1.85	2.37	2.50	1.40	0.40	1.08	0.80
FeO	4.38	3.44	4.85	3.11	3.32	2.69	2.79
MnO	0.19	0.15	0.22	0.11	0.10	0.08	0.08
MgO	5.85	3.96	6.43	3.05	2.36	2.51	2.09
CaO	5.72	4.86	5.59	4.48	4.11	4.10	3.80
Na2O	2.34	3.11	1.96	4.09	4.00	4.21	3.97
K2O	7.02	6.10	5.86	3.53	3.17	3.11	2.79
P2O5	0.37	0.37	0.20	0.30	0.18	0.31	0.25
H2O+	0.54	1.28	0.54	0.47	0.17	0.46	0.64
H2O-	0.29	0.11	0.06	0.15	0.14	0.14	0.05
TOTAL	99.44	100.62	99.91	99.98	99.18	100.94	99.68
Ba	1078		985	429		508	565
Ga	15		15	20		17	19
Pb	61		67	42		32	30
Rb	252		247	213		214	200
Sr	335		225	336		410	344
Th	21		12	21		19	19
U	8		11	16		6	11
Y	18		21	17		21	13
Zr	239		162	236		214	174

Table 2

show strong preferred alignment. This narrow zone grades inwards over a few hundred metres into a more leucocratic adamellite with pink K-feldspar megacrysts up to 50 mm in length. Over a further several kms, the abundance of K-feldspar megacrysts reduces to near zero and where most sparse, are white in colour. In spite of the marked changes in the K-feldspar megacryst abundance, modal K-feldspar (phenocrysts + groundmass) changes little from margin to core. Table 1 gives a selection of analyses for the Macdonald River traverse marked as A-B on Fig 4. and Fig 5 illustrates the modal variation along this traverse.

Small quartz-monzodiorite stocks along the southern and north-western margins of the Walcha Road pluton are sufficiently fine-grained to show that restite-poor magmas of intermediate composition were associated with the Walcha Road pluton. Table 2 lists chemical data for the Back Creek stock, adjoining the pluton to the south, and microgranitoid enclaves of the Walcha Road Pluton.

Like the microstructurally zoned Tuolumne Meadows pluton of the Sierra Nevada Batholith, the zoning within this pluton is suggested to result from sidewall crystallisation of more mafic cumulate rocks with the accumulation of the boundary-layer residual melt near the roof of the magma chamber. Calculations based on pluton shape as deduced from outcrop mapping and K-feldspar foliation measurements indicate that the felsic central parts of the pluton are volumetrically small compared with the more mafic marginal rocks.

THE LOOANGA PLUTON - HOST TO RARE BUT IMPORTANT MICROGRANITOID ENCLAVES.

Sparse microgranitoid enclaves in the Looanga Adamellite near Bendemeer, N.S.W. Australia, range from microdiorite to microgranite and have fine- to medium-grainsize igneous microstructures. The enclaves vary from 53 to 69 per cent SiO_2 and are all less silicic than the host adamellite (73 per cent SiO_2). Although compositionally diverse, the enclaves share several mineralogical and chemical features in common with the host pluton. Both enclaves and pluton contain quartz, oligoclase, variable K-feldspar, ferro-edenitic hornblende and iron-rich (Mg/Mg+Fe 0.37) biotite. The enclaves have low Sr and high U, Th and MnO/(MnO + MgO + FeO) values similar to those of the host pluton although actual MnO

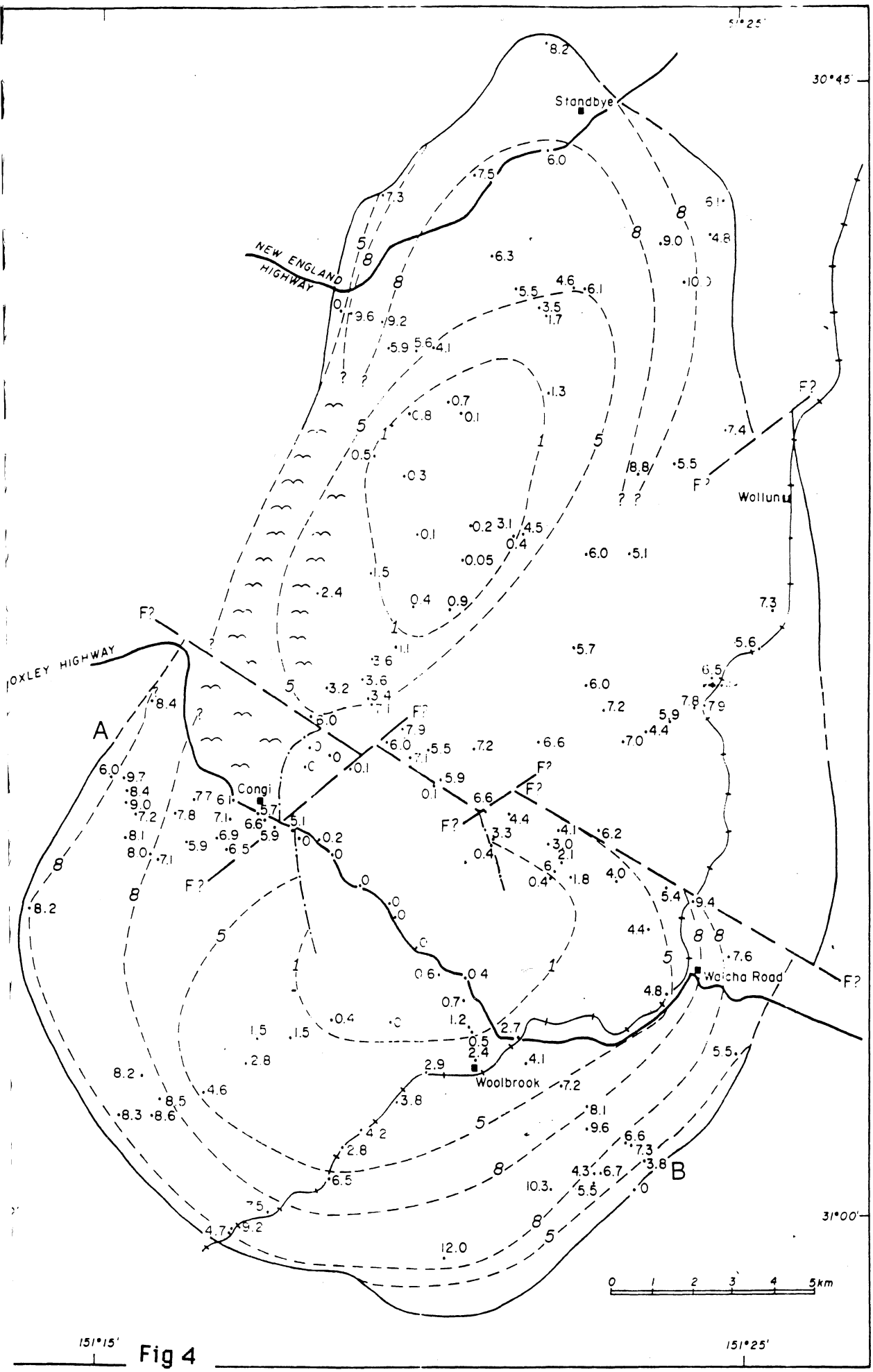

Fig 4

Map of the Walcha Road pluton showing the variation in K-feldspar phenocryst abundance.

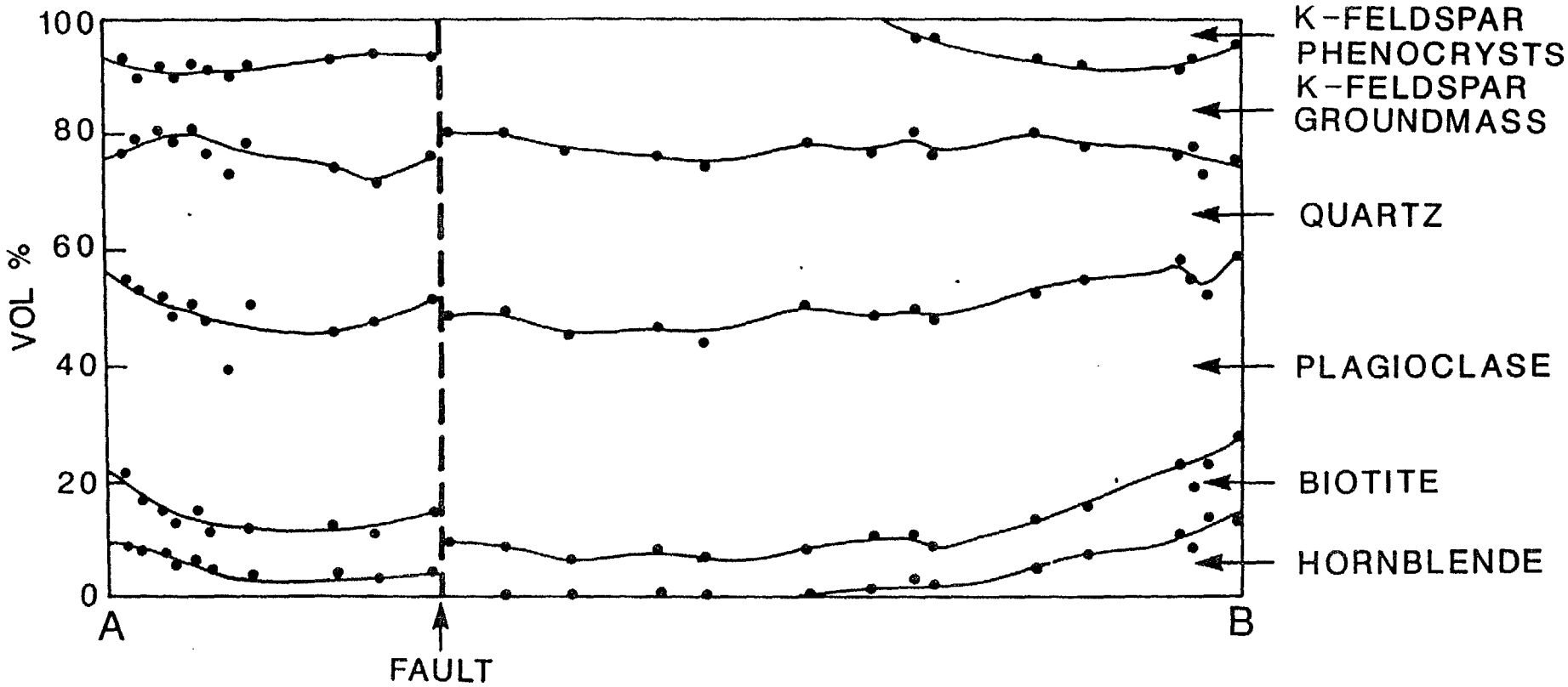

Fig 5 Modal variation across the Walcha Road pluton along line A-B.

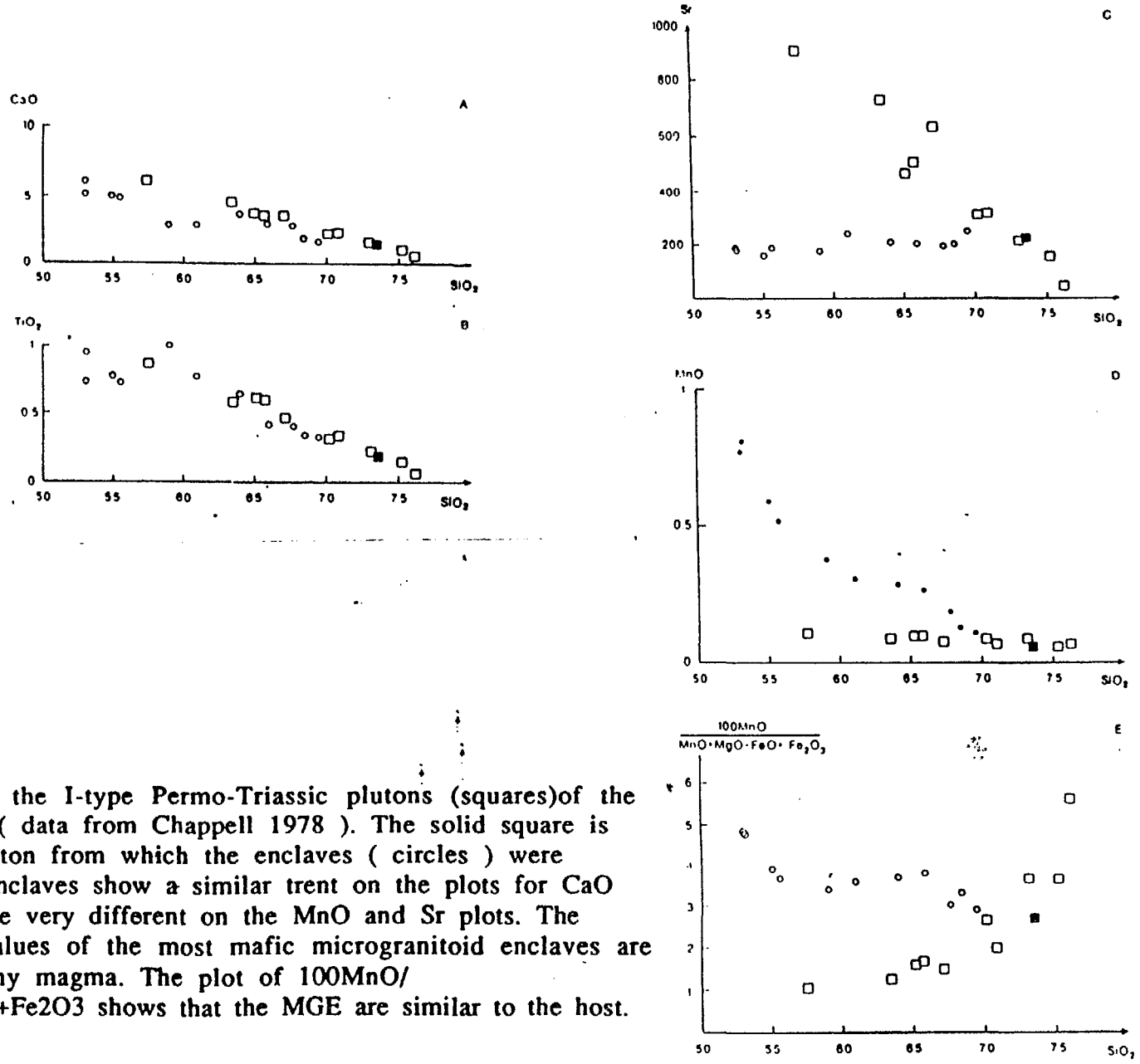

Fig 6

Harker plot for the I-type Permo-Triassic plutons (squares)of the Moonbi district (data from Chappell 1978). The solid square is the Looanga pluton from which the enclaves (circles) were collected. The enclaves show a similar trent on the plots for CaO and TiO2 but are very different on the MnO and Sr plots. The extreme Mno values of the most mafic microgranitoid enclaves are higher than ? any magma. The plot of 100MnO/ MnO+MgO+FeO+Fe2O3 shows that the MGE are similar to the host.

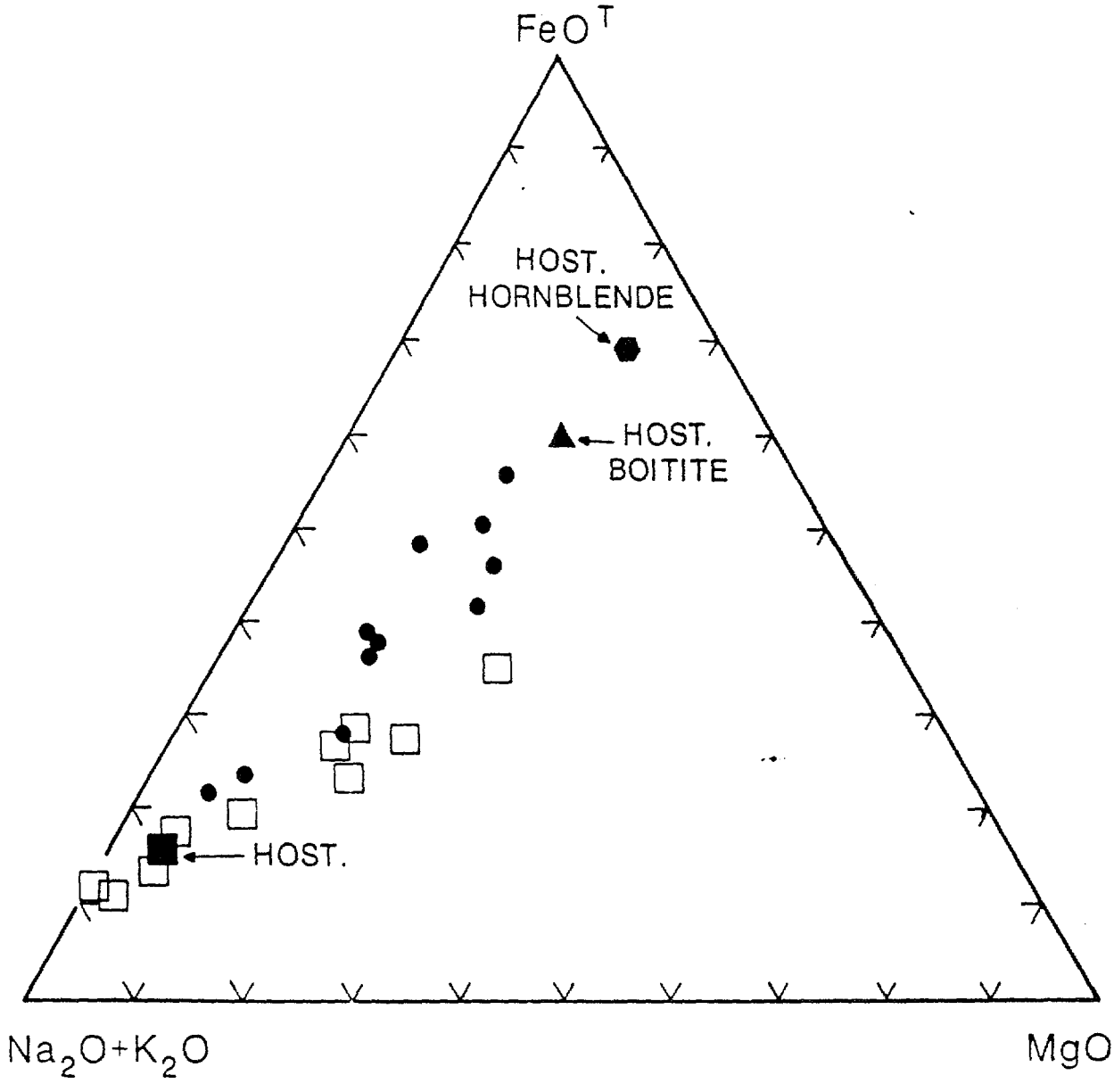

Fig 7

An FMA plot of the I-type Moonbi plutons (squares; data from Chappell 1978) with the MGE from the Looanga pluton (circles) and the composition of the separated biotite and amphibole from the host pluton (filled square). The enclaves can be explained as being cumulates of the mafic minerals of the host pluton.

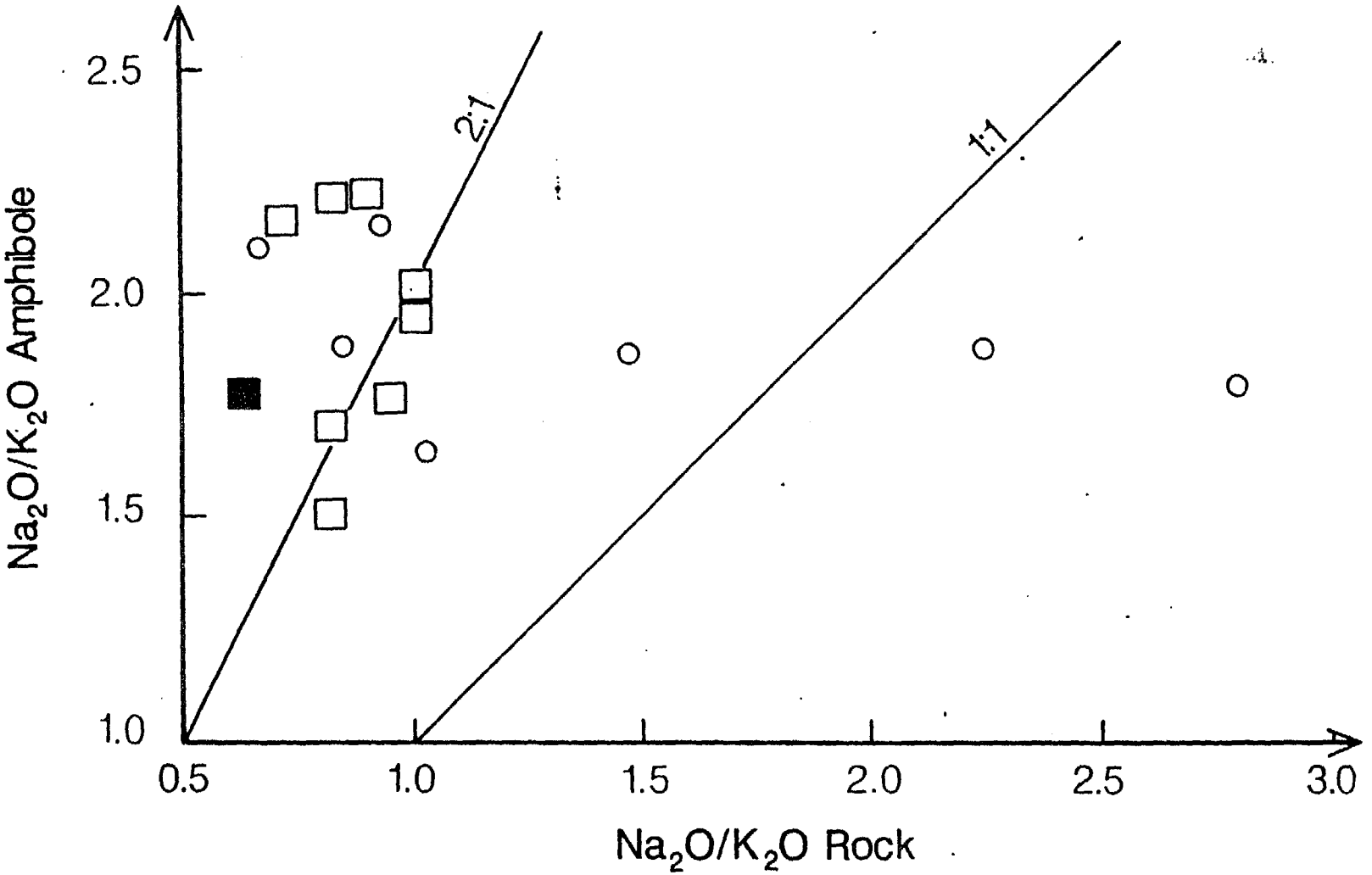
2.5
2.0
1.5
1.0
0.5
1.0
1.5
2.0
2.5
3.0
2:1
1:1
Na_2O/K_2O Amphibole
Na_2O/K_2O Rock

Fig 8

values of the more mafic enclaves are extremely high (up to 0.8 percent). Hornblende and biotite in the enclaves, irrespective of enclave composition, have similar Mg/Fe, Na_2O/K_2O, TiO_2 and MnO contents as those found in the host adamellite and would therefore appear to have crystallised from a magma similar to that of the host. Chemically and mineralogically, the enclaves can be explained as cumulates formed from a magma of similar composition as the host pluton, in that they are enriched in the near-liquidus minerals (amphibole, plagioclase and biotite) and depleted in the near-solidus minerals (quartz and K-feldspar).

The fine-grained microstructure and cumulate chemistry of the enclaves are compatible with a pressure-quench model. Pressure quenching causes a shift of the granite cotectic compositions closer to quartz and K-feldspar with subsequent undersaturaturation of the quenched melt in one or both of these minerals. The enclaves could form as a result of roof or sidewall fracture events that may be minor and short lived but result in the release of a water rich fluid or vapour that forms a barrier between the solid- and melt-rich parts of the magma chamber. As the undercooled melt is now separated from the solid outer part of the pluton by an aqueous fluid phase, heterogenous nucleation takes place on phenocrysts in the melt to form the fine-grained sub-rounded to irregular shaped enclaves. The compositional variety of these enclaves results from the degree of undercooling, the melt compositions available within the zone of undercooling and the effects of increasing temperature due to the heat of crystallisation.

Harker plots of the I-type Moonbi plutons (Chappell 1978) together with the Looanga pluton and its enclaves are shown in Fig 6 . An FMA plot of the same samples (Fig 7), shows that unusual enclave chemistry is explicable in terms of mixing between the bulk-rock and amphibole plus biotite of the host pluton. A plot of amphibole Na2O/K2O vs bulk-rock Na2O/K2O ratios (Fig 8) shows that the amphiboles in the enclaves and the host pluton are similar and not determined by the Na2O/K2O of the enclave.

TUESDAY

2-1 Banalasta Adamellite at Rocky Gully, New England Highway.

2-2 Spring Creek area at "Old Standby". (monzodiorite stock, granofelses and contact metamorphism of the Banalasta Adamellite.

2-3 Contact of the Banalasta Adamellite and country-rock inclusions at "Glenburnie".

2-4 Uralla pluton.
2-5 Balala Dyke Swarm.

THE BUNDARRA SUITE : S-TYPE PLUTONS WITH HIGH SODIUM AND LOW 87Sr/86Sr INITIAL RATIOS (0.706 - 0.707).

These plutons which form a narrow.elongate belt, differ from the Lachlan Fold Belt S-type plutons in that they have low initial ratios and high Na2O. Models that might explain the shape of this narrow continous belt of plutons have been listed by Shaw and Flood (1981). and include: 1) tilting of a tabular body: 2) Formation above a moving "hot-spot": 3) Formation above a linear source. To date no comagmatic volcanic rocks have been identified for this suite of granites.

The Banalasta pluton, the most southern, largest and most mafic of the Bundarra Suite plutons preserves evidence of stoping along its eastern contact with volcaniclastic metasediments. Flood and Shaw (1979) have suggested that the plutons in this region may have been tilted slightly to the east and this would make this eastern contact nearest the roof of the pluton.

The Banalasta pluton is a biotite-cordierite adamellite with rare almandine-rich garnet. The cordierite (average mg of 59 : range 55 to 61), occurs in most but not all Bundarra Suite plutons, is euhedral and magmatic in origin. Some crystals have inclusions of quartz in their centres, but whether the core is a magmatic intergrowth or a restitic core is not clear. The garnet (Flood, Shaw and Chappell; in prep) is zoned from almandine-pyrope-rich cores (Alm68, Pyr25, Spes4, Gros3) to almandine-spessartine-rich rims (Alm74, Pyr11, Spes13, Gros2). These igneous garnets contrast with the largely metamorphic garnets of the Cowra pluton which are zoned from manganese-rich cores to almandine-rich rims, Fig 9 (from unpublished data of Flood , Shaw and Chappell). The very leucocratic plutons of the Bundarra suite commonly have rapakivi feldspar especially in the more porphyritic finer-grained margins.

The Bendemeer and Looanga plutons of the Moonbi Suite have intruded the late Carboniferous Bundarra Suite and have produced metamorphic effects in the older granites. Clare (1989) has recognised two zones within the metagranites on the basis of K-feldspar triclinicity (Fig 10).
1) A high-grade zone that is contact parallel and extends approximately 2 km into the Banalasta pluton. The zone is

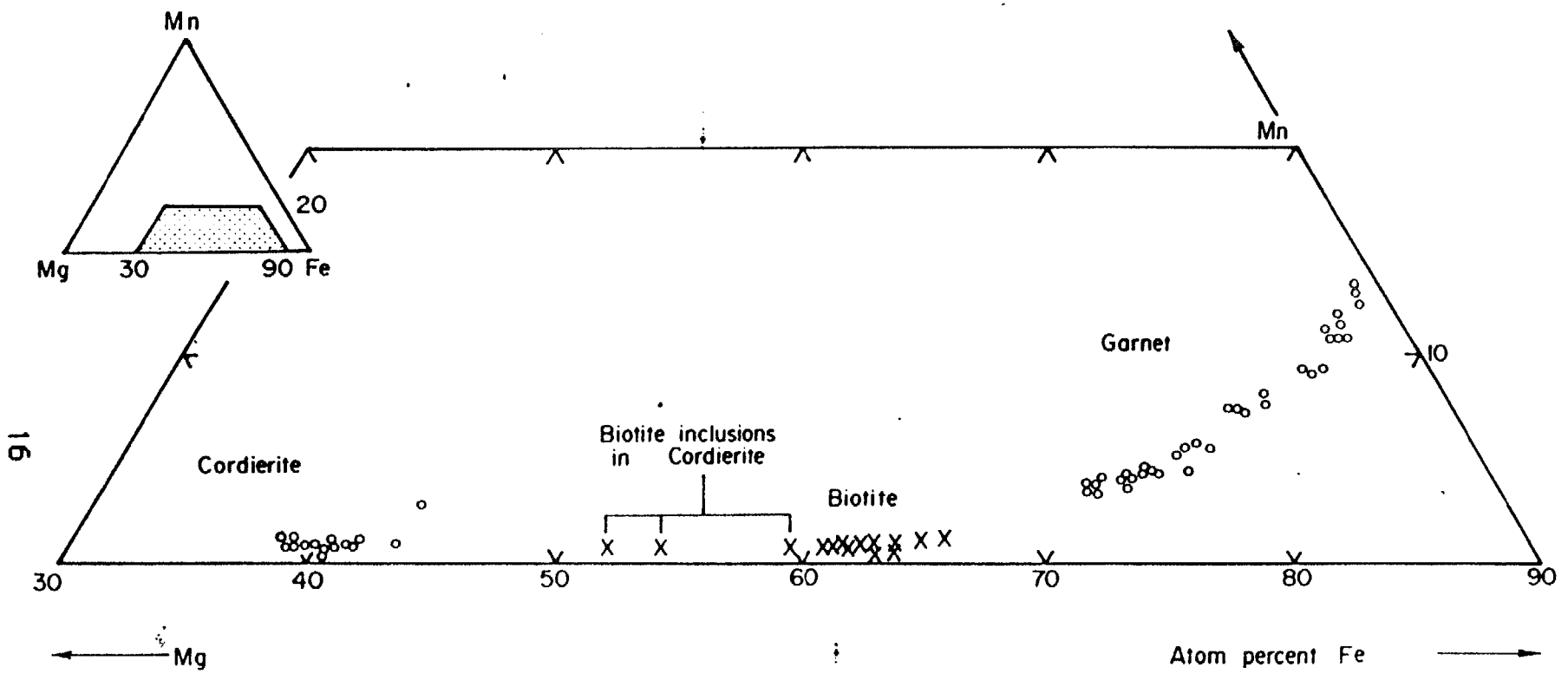
Mn
20
Mg
30
90 Fe
Mn
Garnet
10
Cordierite
Biotite inclusions
in Cordierite
Biotite
10
30
40
50
60
70
80
90
Mg
Atom percent Fe

Fig 9

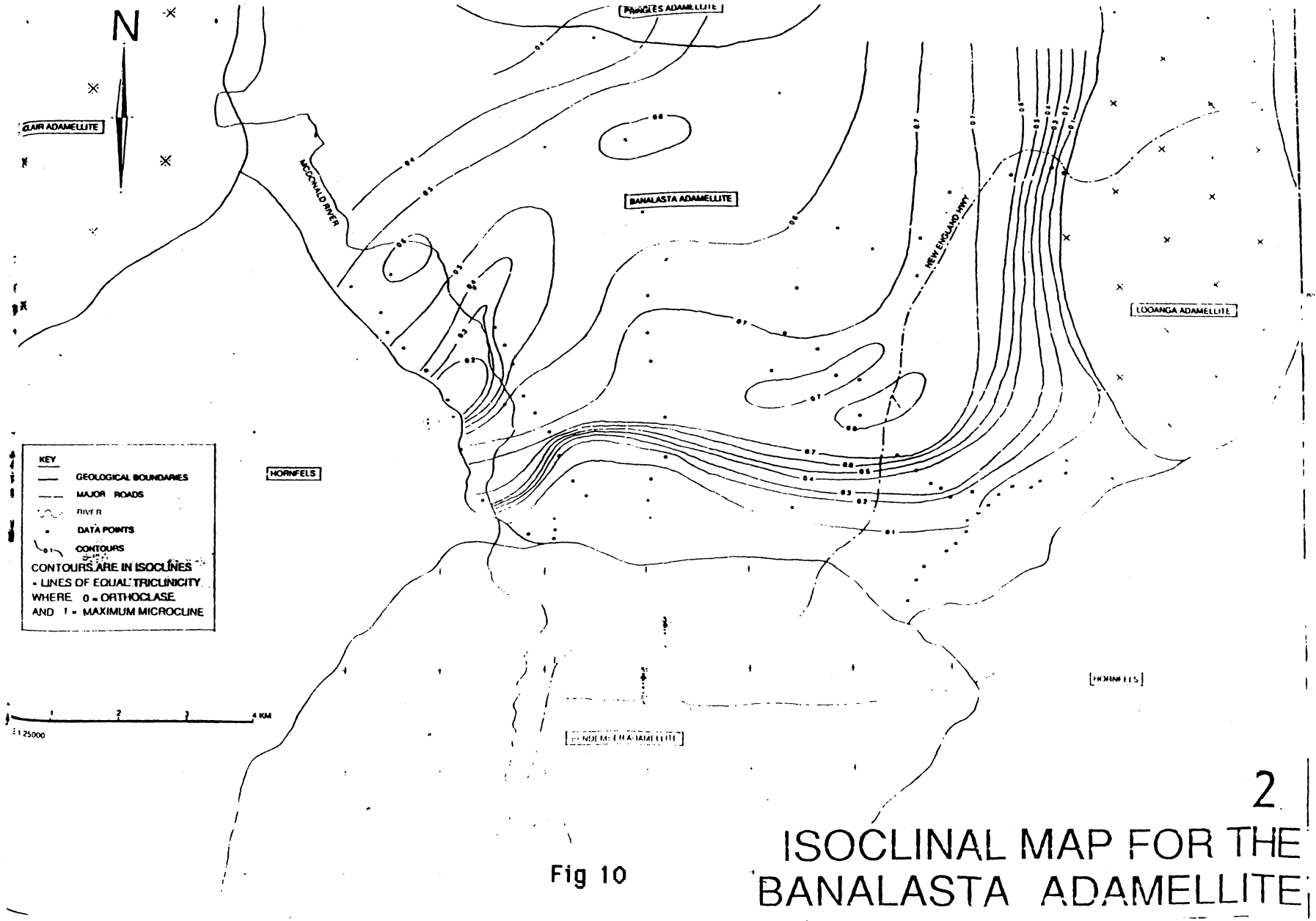

Fig 10

2

ISOCLINAL MAP FOR THE BANALASTA ADAMELLITE

characterised by disordered K-feldspar (ie low triclinicity) and microstructural evidence of recrystallization.
2) A low-grade zone having a relatively sharp contact with the high-grade zone extends as far as four km from the contact. This zone is characterised by K-feldspar that is much more ordered (high triclinicity) than K-feldspar of the Bundarra Suite away from the younger plutons. The zone also exhibits evidence of minor ductile and brittle strain of quartz , plagioclase and biotite. Clare(1989) from careful documentation of these metamorphic zones, has located an anomolous area of low triclinicity just north of Bendemeer that may indicate a blind pluton. The method of triclinicity zonation could have general application in determining the order of intrusion of adjacent granites. Within the aureole of the Bendemeer pluton, magmatic cordierite of the Banalasta pluton is replaced at the lowest grades by an isotropic chlorite, at higher grades by muscovite and chlorite and at the highest grades by aggregates that include andalusite and metamorphic cordierite.

THE BALALA DYKE SWARM

This large dyke swarm that indicates a signifigant extension of the upper crust in the late Permian (Fig 11) is largely confined to the Yarrowyck and Balala Granodiorites with just a few extending south into the Uralla pluton and the metasedimentary rocks. Both the Yarrowyck Granodiorite and the dyke swarm are truncated by the Gwydir River pluton. The dykes have a wide range of compositions as shown by Thompson (1989
) (Table 3) but with the majority being of dacitic and rhyolitic composition.

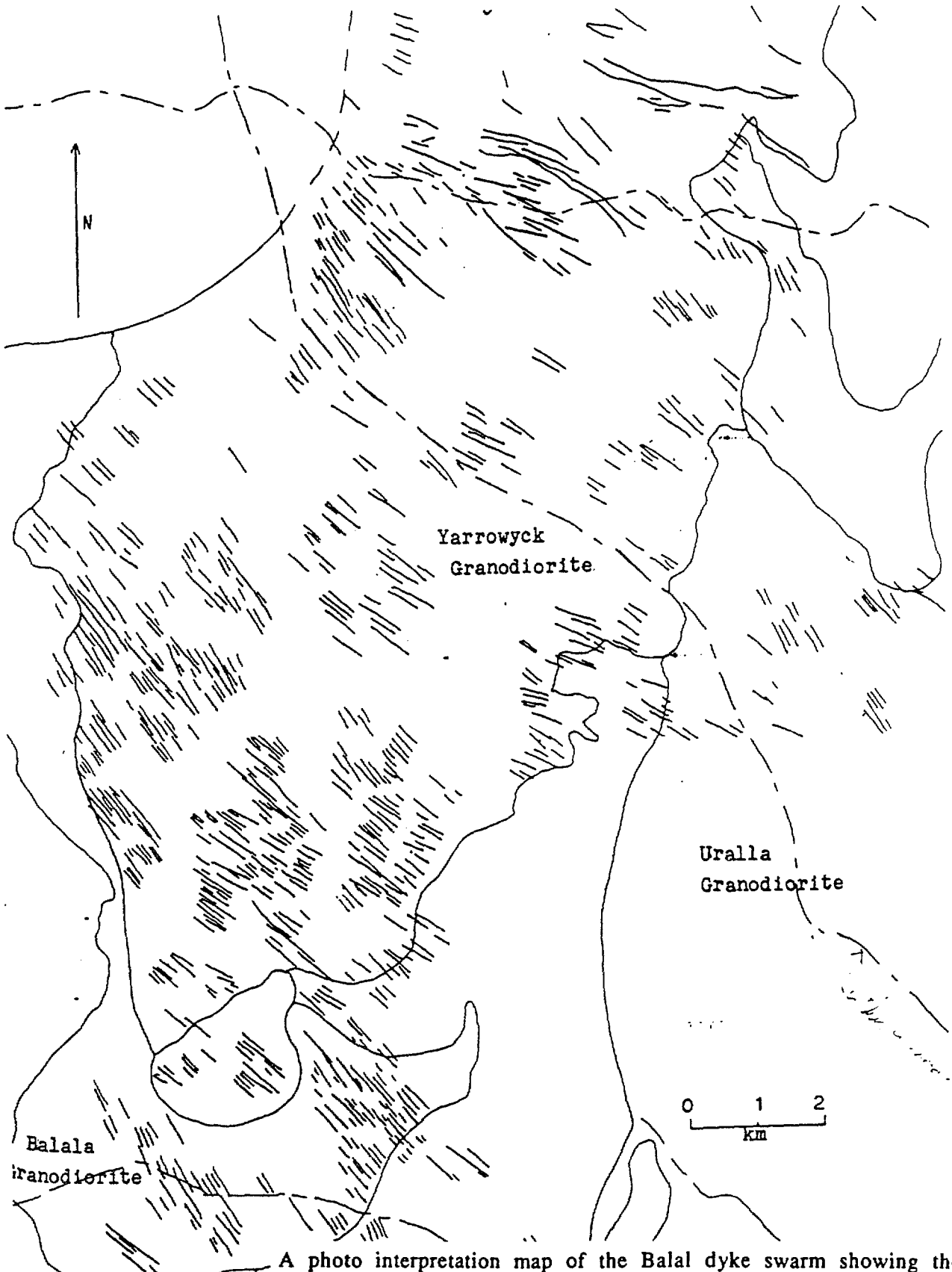

Fig 11 A photo interpretation map of the Balal dyke swarm showing the concentration in the Yarrowyck Granodiorite and Balala Granodiorite with a few in the northern part of the Uralla pluton. The Gwydir River Adamellite truncates both the Yarrowyck Granodiorite and the dyke swarm.

Spec No.	BDN4	JRT	BDN6	BDN2	BDN3	JRR
SiO2	55.38	59.11	59.49	59.79	68.35	75.23
TiO2	0.94	0.93	0.74	0.77	0.48	0.08
Al2O3	15.73	16.56	15.00	13.94	15.38	12.27
Fe2O3	1.82	1.13	1.13	1.73	0.40	0.03
FeO	4.90	5.03	4.65	4.28	2.90	0.62
MnO	0.14	0.11	0.12	0.13	0.08	0.04
MgO	5.84	4.14	5.25	7.26	1.62	0.16
CaO	7.11	7.04	5.87	5.67	3.00	1.39
Na2O	3.52	3.85	3.53	2.90	4.15	2.98
K2O	2.10	2.00	2.67	3.09	3.87	5.78
P2O5	0.16	0.18	0.14	0.17	0.16	0.03
H2O+	1.08	0.03	1.11	0.69	0.35	0.73
H2O−	0.34	0.18	0.20	0.11	0.12	0.17
Total	99.06	98.82	99.90	100.53	100.86	99.51
Q	23.20	7.70	8.12	8.57	19.46	32.97
Or	0.95	11.82	15.77	18.26	22.86	34.15
Ab	15.73	32.56	29.86	24.53	35.10	25.20
An	17.46	22.00	17.20	15.90	11.92	3.04
C	6.10	0.00	0.00	0.00	0.00	0.00
Di	0.00	9.59	8.91	8.88	1.59	2.84
Wo	0.00	0.00	0.00	0.00	0.00	0.14
Hy	24.59	12.59	15.36	19.23	7.59	0.00
Mt	2.64	1.64	1.64	2.51	0.58	0.04
Il	1.79	1.77	1.41	1.46	0.91	0.15
Ap	0.00	0.42	0.32	0.39	0.37	0.07

Analyses of five of the Balala dyke swarm from Flood 1971 and Ransley 1970.

Table 3

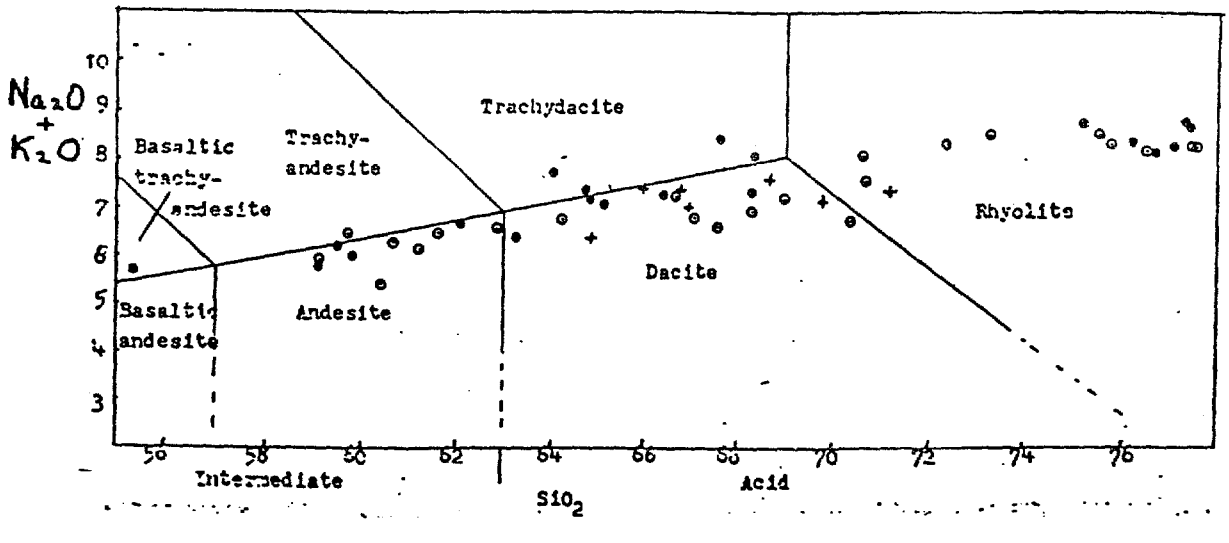

Fig 12 Plot of many analyses of the Balala dykes from Thompson on the Le Bas plot showing both the range of compositions.

STRUCTURAL AND METAMORPHIC EVOLUTION OF THE WONGWIBINDA METAMORPHIC COMPLEX

T.R.Farrell
Department of Geology, University of Newcastle

WEDNESDAY

The Wongwibinda Metamorphic Complex, in the southern New England Fold Belt, is a small, low-P/high-T terrain associated with the Abroi Granodiorite, a member of the Hillgrove Plutonic Suite. The complex is bounded in the north by the Wards Mistake (I-type) and the Kookabookra (S-type) Adamellites, and in the east by the Wongwibinda Fault, a major structural element of the New England Fold Belt. In the south and west there is no well defined border (cf. Binns, 1966) but rather there is a transition from low grade rocks (sub-biotite grade) in the Girrakool area 12km to the southwest, through to upper amphibolite facies schists at Wongwibinda. A notable feature of the Complex is the rapid progression, over a remarkably short distance, from fine grained low grade schists in the west to high grade schists, migmatites and syn-tectonic S-type granitoids in the core of the complex.

The complex comprises a sequence of fine-grained, pelitic and psammo-pelitic schists (Rampsbeck Schists; Binns, 1966), with sporadic thin lenses and layers of calc-silicate, and minor amphibolites and quartzites (Stephenson and Hensel 1979, 1981). These rocks are interpreted to be a deformed and metamorphosed accretionary sequence. The lower grade Rampsbeck Schists (lower amphibolite facies) are fine grained rocks containing quartz, biotite, plagioclase and muscovite. Various sedimentary structures (graded bedding, load casts, cross bedding) are still recognisable. In some locations, highly disrupted bedding contacts showing delicate flame-shaped or bulbous contacts, and very irregular folds with thrust faults and fine wispy axial plane injections of pelitic material are evidence for deformation of the sediments in an unconsolidated state, either during deposition or shortly afterwards in subduction and accretion.

High grade Rampsbeck schists are coarser grained and contain quartz, plagioclase, K-feldspar and biotite, as well as cordierite, garnet and sillimanite in more pelitic varieties. The peak conditions of metamorphism have been estimated at 650-675°C and 2.8-3.4 kbar from garnet-biotite thermometry and plagioclase-garnet-muscovite-biotite barometry. The schists are transitional into a zone of migmatites in which the rocks contain numerous thin, closely spaced, parallel quartz-rich veins and are intruded by irregular coarse grained granitic leucosomes. At the highest metamorphic grades (upper amphibolite facies) pelitic migmatites are intruded by small bodies of peraluminous cordierite-muscovite granitoid.

The Abroi Granodiorite (Binns, 1966), an elongate, deformed S-type pluton, lies along the eastern margin of the Complex. The Abroi is relatively biotite-rich (up to 19 vol%) and contains minor amounts of myrmekite, occasionally garnet, and accessory ilmenite, sphene and apatite. It has abundant metasedimentary (schist and calc-silicate) and minor mafic enclaves, and relict quartz veins and pegmatites, and is intruded by syn-genetic aplitic dykes. Along the Wongwibinda Fault the Abroi is mylonitised in a wide zone (up to 1.6km in width), and thrust over the low-grade Dyamberin Beds (Binns, 1966) to the east.

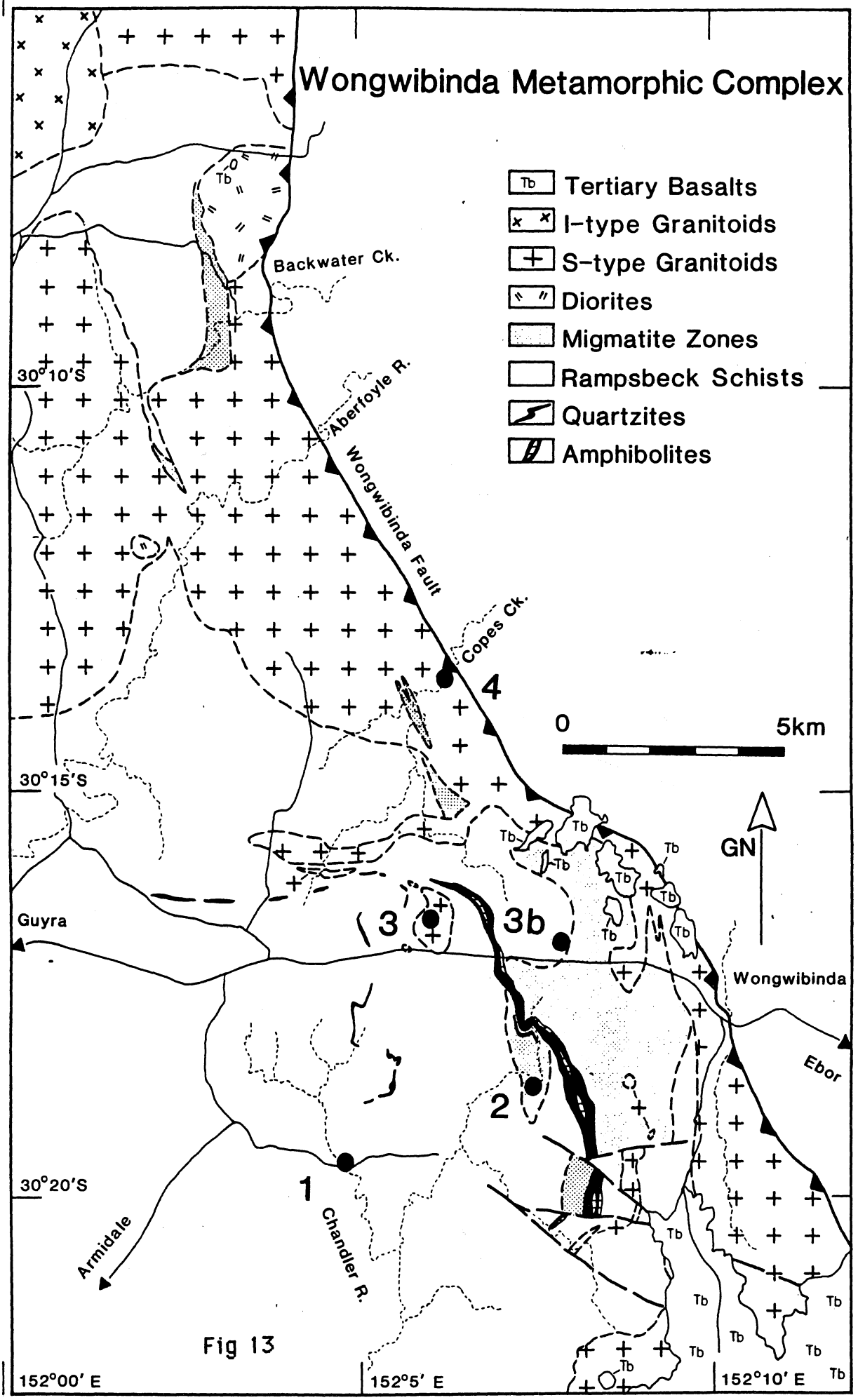
Wongwibinda Metamorphic Complex
Tb Tertiary Basalts
I-type Granitoids
S-type Granitoids
Diorites
Migmatite Zones
Rampsbeck Schists
Quartzites
Amphibolites
Backwater Ck.
Aberfoyle R.
Wongwibinda Fault
Copes Ck.
30°10'S
30°15'S
30°20'S
0
5km
GN
Guyra
Wongwibinda
Ebor
Armidale
Chandler R.
1
2
3
3b
4
Tb
152°00' E
152°5' E
152°10' E

Fig 13

STRUCTURAL GEOLOGY

The rocks of the Wongwibinda Complex show evidence of four phases of deformation (D_1-D_4; Farrell, 1988), recognised on the basis of the overprinting of foliations and small scale folds. D_1 was an intense, pervasive deformation, coeval with amphibolite facies metamorphism and migmatisation, that produced steeply plunging, open to isoclinal folds (F_1), an associated axial plane foliation (S_1), and very strong lateral extension. The effects of D_1 are recognisable throughout the complex but are most pronounced in the higher grade rocks. Extension parallel to F_1 axes is particularly strong and rootless, isoclinal, intrafolial folds, and boudinaged pegmatites and calc-silicates are common. In contrast to the first deformation, D_2 resulted in very heterogeneous strain, characterised by the buckling and "transposition" of pre-existing structures. It produced steeply plunging, gentle to isoclinal, typically asymmetric folds (F_2) with an axial plane schistosity (S_2), and was associated with amphibolite facies metamorphism and the generation of granitic melts. D_3 was an episode of heterogeneous non-coaxial, simple shear that resulted in the formation of Type I S-C mylonites (Lister and Snoke, 1986) in the Wongwibinda, Glen Bluff and associated minor shear zones. D_3 features are best developed in discrete shear zones in granitic rocks, although migmatites, schists and quartzites close to these zones may also show evidence of shearing. The first effects of shearing are observed in granitoids up to 1.6km from the Fault with the incipient development of lineated shear planes (C) which deflect a pre-existing, weakly developed foliation (S). Approaching the Wongwibinda Fault the shear planes (C) become more pervasive, continuous and closely spaced, S-planes are more strongly developed, and the S-C angle decreases from about 40° initially, to 0-10° adjacent to the fault. In the most intensely deformed rocks C'-planes and thin ultramylonite bands are developed. S-C relationships, asymmetric augen, mica fish and displaced broken grains, all consistently indicate a west over east, reverse sense of movement on the Wongwibinda Shear Zone. The stretching lineation (L_3), dips steeply to the west or westsouthwest, indicating an east to eastnortheast direction of thrusting. The final deformation, D_4 was a minor event that produced kinking of pre-existing structures.

MIGMATITE GENESIS

Migmatites in the Wongwibinda Metamorphic Complex show evidence of progressive development during prograde metamorphism in D_1 and D_2. First generation (D_1) leucosomes are generally thin, occur sub-parallel to S_1 and are quartz-rich. Two distinct types are present: thin vein-like leucosomes (< 5mm thick) with very high length/width ratios (100-200), and thicker leucosomes (up to 50mm thick) which are boudinaged in S_1 and commonly have a pod-like or lenticular shape. The former are typically closely spaced, have relatively constant modal compositions (qtz 45-50%, plg 35-40%, kfs 5-12%, bio 1-8%), and become progressively thicker with increasing degree of migmatisation. The lenticular leucosomes are interpreted to be early D_1 features because of their strong but variable extension in S_1. They are frequently linked by thin quartz-rich veinlets, and contain variable amounts of quartz (45-90%) and feldspar (plg 4-50%, kfs 0-17%). A second generation of thicker, coarser grained, variably deformed "granitic" leucosomes crosscuts the D_1 leucosomes. Compositionally, these later leucosomes range from leuco-adamellite, with sub-equal proportions of plagioclase and K-feldspar, to biotite-granodiorite (up to 13% bio). They appear to have formed at all stages of D_2: early leucosomes cut S_1 but are folded about S_2, whereas late stage leucosomes are relatively straight and lie parallel to S_2. Leucocratic leucosomes usually have very sharp

discordant boundaries, irrespective of the timing of their formation, but biotite-rich leucosomes often have diffuse margins and ghost fabrics concordant with S_1 in the host schist. Coarse grained pegmatitic varieties are relatively straight, occur parallel to the axial surfaces of F_2 folds, have sharp discordant boundaries and are interpreted to be late D_2 features.

D_1 and D_2 leucosomes are geochemically distinct. As a consequence of their quartz-rich compositions D_1 leucosomes are strongly depleted in a wide range of trace elements (eg. Rb, Ba, Hf, Th, Zr, Y, LREE) with respect to their host rocks. In contrast, biotite-rich leucosomes display incompatible element contents which are remarkably similar to those of the host rock.

The chemistry and structural relationships indicate that D_1 leucosomes formed under sub-solidus conditions; their mineralogy deviates significantly from minimum melt compositions, they are typically extended in S_1, implying solid state deformation during D_1, and their depleted incompatible trace element compositions are not consistent with an anatectic origin. Conversely, the textural relationships suggest that D_2 leucosomes formed by anatectic processes. Biotite-granodiorite leucosomes with gradational margins are interpreted to be partial melts that have not segregated from their source but have frozen in situ (sensu lato). This can account for the presence of vague internal structures which are continuous with S_1 in the host rock, and the remarkable similarity of the trace element composition of the host and leucosome. Leuco-adamellite leucosomes are thought to be partial melts that formed at deeper levels and intruded upwards into the overlying migmatites.

FIELD STOPS

The purpose of this field excursion is three-fold: i) to look at the progression from low grade schists through to migmatites and granites, ii) to evaluate the time relationships between deformation and melting, and iii) to examine ductile shear fabrics in the Abroi Granodiorite indicative of uplift on the Wongwibinda Fault.

Stop no.1: Low grade schists, Chandler River

At this location the rocks consist of interbedded mudstones and quartz-bearing greywackes that have been recrystallised into fine grained schists. They have only been affected by one deformational event which produced the weakly developed cleavage. These rocks are the low grade equivalents of the migmatised and deformed rocks in the core of the complex. Graded bedding and load casts are recognisable and they indicate that the sequence is overturned and faces to the west. These rocks are interpreted to be a coherent turbidite sequence, possibly deposited in a trench-slope setting.

Stop no.2: High grade schists and migmatites, Spring Creek

The high grade schists and migmatites at this location are noticeably coarser grained than the low grade rocks at stop number one, although bedding is still recognisable. The rocks have been intensely folded during D_2 to produce some superb ptygmatic structures in thin leucosomes and tight, typically asymmetric folds in bedding. Stromatic (layered) migmatites are well developed - the rocks contain numerous thin S_1 parallel leucosomes. Crosscutting the D_1 structures are a series of syn-D_2 leucosomes, many of which are sub-parallel to S_2.

Many biotite-rich D_2 leucosomes display gradational margins, indicating that melting had not proceeded far enough to allow the melt segregate from the source area. Folded lenses of zoned calc-silicate are also present; they are interpreted to be the boudinaged remnants of former thin calcareous layers.

Stop no.3: Pelitic migmatites and peraluminous granitoids, Rock Abbey

At this location a strongly peraluminous granitoid contains a range of metasedimentary enclaves from abundant small schlieren through to large rafts of pelitic migmatite. The migmatites record the structural history of the rocks up until substantial melting took place: they contain recognisable bedding, refolded F_1 folds, and F_2 folded D_1 stromatic leucosomes. The structural relationships shown by the migmatites indicate that granitoid formation took place late in D_2 (cf. Stephenson & Korsch, 1976; Korsch, 1981) - many enclaves display F_2 folding of S_1, granitic melt has been intruded along the axial plane of F_2 folds, and many of the granitic pods display a weak foliation which is parallel to the axial plane of F_2 folds in adjacent schistose blocks.

Compositionally, the granitoids are biotite-muscovite adamellites and they contain minor retrogressed cordierite and accessory ilmenite and tourmaline. The coexistence of muscovite and quartz indicates that crystallisation took place at pressures above that of the invariant point defined by the intersection of the haplogranite solidus and the quartz + muscovite breakdown reaction. The presence of cordierite additionally constrains the crystallisation pressure to have been very close to the invariant point ie. about 3-4kbar.

Stop no. 3b: (Optional) High grade schists, The Range

The high grade schists at this location contain abundant thin leucosomes and show very good development of F_2 folds. Also developed parallel to S_2 are some thicker granitic leucosomes. The heterogeneity of the strain associated with D_2 is apparent: in high strain zones S_1 is completely transposed into S_2 orientations; whereas in low strain areas S_1 displays open F_2 folding. A large dextral D_4 kink band folds the transposed S_1 fabrics. Also apparent is asymmetric extension of bedding.

Stop no.4: Mylonitised Abroi Granodiorite, Wongwibinda Fault

This locality shows the very strong deformation associated with ductile shearing along the Wongwibinda Shear Zone. S-C fabrics, mineral stretching lineations and asymmetric microstructures are exceptionally well developed. The S-C angular relationships and the asymmetry of feldspar porphyroclasts and biotite "fish" are consistent with reverse movement on the Wongwibinda Fault. A high shear strain (= 4-5) is indicated by the low angle between S and C (0-10°) and by the development of late shear bands (C') and numerous thin ultramylonite bands. The ultramylonites are generally parallel to C but some are discordant. Also present at this locality are folded and sheared pegmatites and a post-D_3 mafic dyke. The mafic dyke is largely concordant with D_3 fabrics although it displays some local discordance, and at one point it has stoped off a fragment of the Abroi containing S-C fabrics.

References

Binns R.A. 1966 Granitic intrusions and regional metamorphism of Permian age from the Wongwibinda Complex, north-eastern New South Wales. Journal and Proceedings of the Royal Society of New South Wales **99**, 5-36.

Farrell T.R. 1988 Structural geology and tectonic development of the Wongwibinda Metamorphic Complex, in Kleeman J.D. (ed.) New England Orogen: tectonics and metallogenesis, Department of Geology and Geophysics, University of New England, 117-124.

Korsch R.J. 1981 Structural geology of the Rockvale Block, northern New South Wales. Journal of the Geological Society of Australia **28**, 51-70.

Lister G.S. & Snoke A.W. 1984 S-C Mylonites. Journal of Structural Geology **6**, 617-638.

Stephenson N.C.N. & Korsch R.J. 1976 The Wongwibinda complex, northern New South Wales. Excursion Guide 16A, 25th International Geological Congress, Sydney, 38-41.

Stephenson N.C.N. & Hensel H.D. 1979 Intergrown calcic and Fe-Mg amphiboles from the Wongwibinda Metamorphic Complex, N.S.W., Australia. Canadian Mineralogist **17**, 11-23.

Stephenson N.C.N. & Hensel H.D. 1981 Amphibolites and related rocks from the Wongwibinda Metamorphic Complex, northern N.S.W., Australia. Lithos **15**, 59-75.

THURSDAY
THE URALLA CENTRE : A VOLCANIC-PLUTONIC CENTRE
Stops
4-1 the Terrible Vale - Metagranite contact
4-2 the southern margin of the Terrible Vale pluton
4-3 the Kentucky diorite, enclaves and xenoliths
4-4 the Terrible Vale - Harnham Hill Volcanics contact
4-5 the Uralla pluton at Thunderbolts Rock.
4-6 the Uralla pluton at the quarry in Uralla.

The Late Permian Uralla Igneous Centre (see map Fig 14) consists of a series of andesitic and pyroclastic flows (Harnham Hill volcanic rocks), the Terrible Vale intrusive rocks, the Uralla Granodiorite and the Kentucky Diorite. It is probable that the Yarrowyck Granodiorite to the northwest of the Uralla pluton is also part of the Centre. All the late Permian volcanic rocks that are comagmatic with the New England Batholith have been recently named the Wandsworth Volcanics by Barnes et al. 1991.

The Harnham Hill volcanic rocks comprising mainly andesites together with the underlying sedimentary rocks that outcrop just to the east of Kentucky are intruded by the Terrible Vale rocks, a microstructurally zoned facies that vary from dacite to quartz monzodiorite and these in turn are cross-cut by the Uralla Granodiorite pluton to the north west. An extension of the andesites and Terrible Vale rocks outcrop to the northwest of the Uralla pluton. The preservation of the andesites and thermally metamorphosed sedimentary rocks partly encompassed by the Terrible Vale rocks suggests they are down-faulted blocks within a cauldera. The Terrible Vale facies at Kentucky South are intruded by the coarser-grained and more mafic Kentucky Diorite and to the south-west are separated by a narrow screen of hornfels from the younger Walcha Road Adamellite.
The Terrible Vale facies along their contact margins are two-pyroxene dacite tuffisites with fragmental microstructures superficially similar to many ignimbrites. The tufficites are considered to have been feeder zones for one or more major ignimbrite eruptions, the products of which have since been removed by erosion. They exibit a seemingly transitional microstructural change inward from the fragmental two-pyroxene dacite to a fine-grained porphyritic- through medium-grained to coarse-grained near-equigranular quartz monzodiorite.

The andesites, dacite and quartz monzodiorite share strong chemical and isotopic similarities with the Uralla pluton (I-type

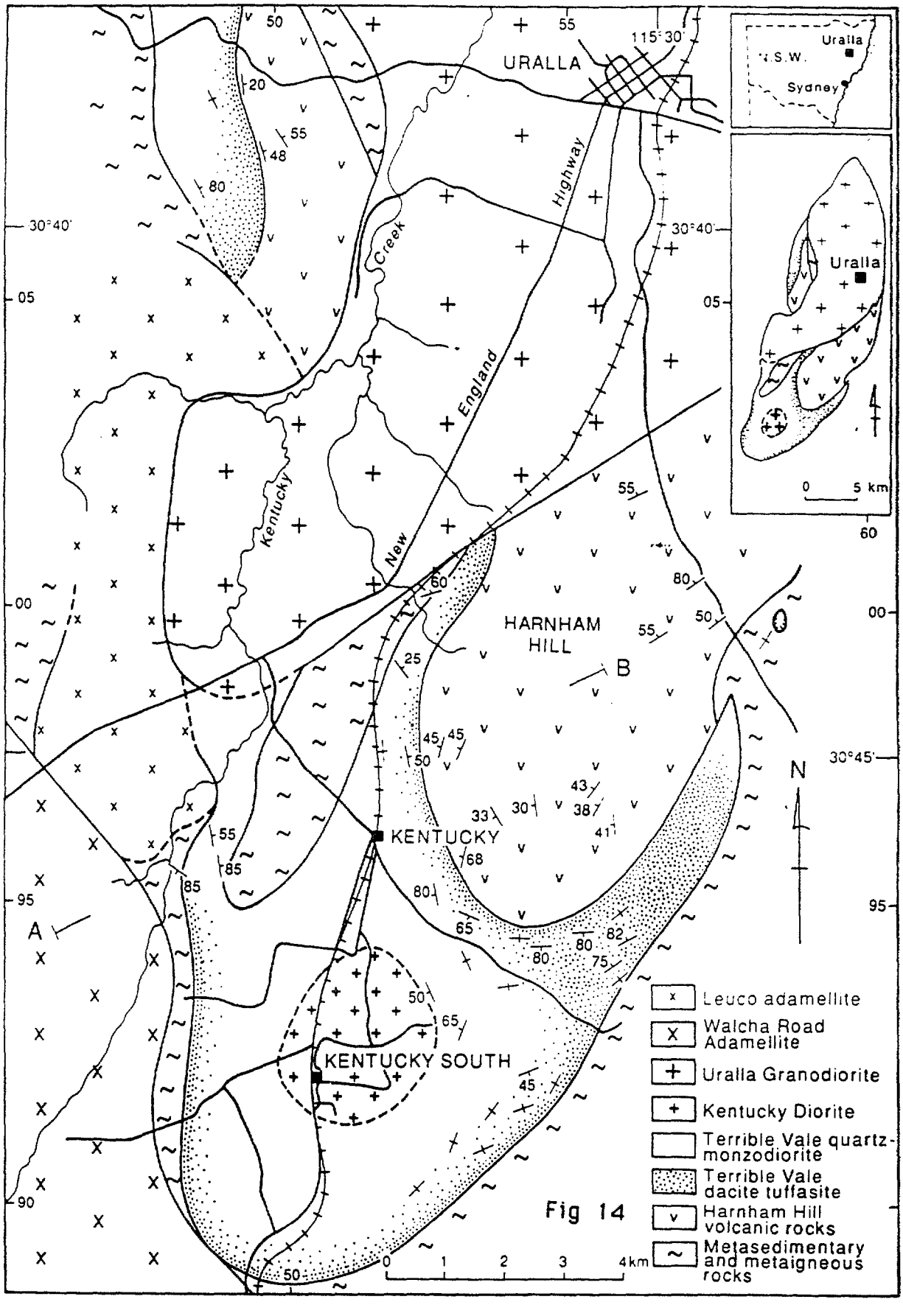
URALLA
115°30'
Uralla
N.S.W.
Sydney
Uralla
0 5 km
Highway
Creek
England
Kentucky
New
HARNHAM HILL
KENTUCKY
KENTUCKY SOUTH
A
B
30°40'
30°45'
N
0 1 2 3 4km
Leuco adamellite
Walcha Road Adamellite
Uralla Granodiorite
Kentucky Diorite
Terrible Vale quartz-monzodiorite
Terrible Vale dacite tuffasite
Harnham Hill volcanic rocks
Metasedimentary and metaigneous rocks

Fig 14

	Terrible Vale dacite tuffasite					Terrible Vale quartz monzodiorite					Uralla pluton			Kentucky pluton	
	1	2	3	4	5	6	7	8	9	10	11	12	13	14	15
	FS2046	FS1800	FS1839	FS1777	FS1930	FS1927	FS1969	FS1906	FS1950	FS1933	WCR	FS941	UQ	DA2	DA1
SiO2	64.26	64.35	64.56	64.83	65.13	63.76	64.08	64.27	64.49	64.63	61.20	65.05	67.10	47.80	52.92
TiO2	0.64	0.65	0.67	0.64	0.65	0.64	0.64	0.66	0.64	0.64	0.78	0.66	0.55	1.91	1.37
Al2O3	15.05	14.88	15.12	14.79	14.79	14.63	14.97	14.77	14.93	14.97	14.77	14.58	14.13	12.78	14.79
Fe2O3	0.96	1.33	1.00	1.01	1.07	0.75	0.74	0.95	1.02	0.92	0.77	0.54	0.79	2.50	1.52
FeO	4.07	3.66	3.85	3.62	3.54	3.94	3.95	3.68	3.68	3.77	4.79	3.92	2.91	8.37	7.15
MnO	0.11	0.10	0.24	0.12	0.09	0.10	0.09	0.08	0.08	0.07	0.18	0.09	0.08	0.23	0.19
MgO	3.82	3.90	3.68	3.62	3.42	3.54	3.82	3.76	3.54	3.56	4.93	3.03	2.56	10.69	8.02
CaO	4.32	4.22	4.22	4.05	4.00	4.08	4.04	4.08	4.06	4.12	4.74	3.95	3.15	9.27	7.41
Na2O	3.04	3.11	3.11	3.03	3.09	3.01	3.12	3.11	3.06	3.12	2.85	2.85	3.39	1.55	2.51
K2O	3.27	3.33	3.33	3.48	3.50	3.39	3.40	3.35	3.38	3.31	2.96	3.49	4.12	2.99	2.64
P2O5	0.23	0.21	0.20	0.20	0.20	0.19	0.18	0.20	0.19	0.21	0.25	0.20	0.15	0.74	0.38
H2O+	0.51	0.13	0.21	0.22	0.21	0.73	0.72	0.68	0.13	0.65	1.47	1.08	0.30	0.68	
H2O-	0.09	0.25	0.29	0.40	0.27	0.26	0.10	0.25	0.06	0.00	0.08	0.11	0.23	0.47	
CO2	0.00	0.08	0.07	0.15	0.30	0.17	0.17	0.13	0.10	0.07	0.20				
TOTAL	100.37	100.20	100.55	100.16	100.26	99.19	100.02	99.97	99.36	100.04	99.97	99.55	99.46	99.98	98.90
Ba	744	733	719	753	778	750	743	746	736	706	853	735	611	1264	1301
Cr	196	198	195	183	184	217	213	209	211	204	305	226			
Cu	24	30	23	31	25	22	23	23	28	20	25	23			
Ga	16	19	19	19	18	15	15	21	21	19	16	19	17	18	20
Nb	9	8	9	9	11	11	10	11	8	9	10				
Ni	45	43	41	41	39	41	39	39	38	39	70	36			
Pb	27	19	19	23	21	21	22	19	21	23	22	22	19	5	21
Rb	138	141	142	153	154	139	139	140	141	137	110	127	174	141	126
Sr	329	325	320	315	310	318	309	315	307	324	367	300	271	422	500
Th	19	15	16	19	17	14	16	19	19	18	14	19	28	5	8
U	6	7	6	8	7	4	8	1	7	9	6	3	11	3	3
V	87	91	95	82	85	90	83	97	89	90	113	80			
Y	26	30	32	32	25	30	32	29	29	31	25	26	25	31	25
Zn	66	63	66	60	59	70	69	67	65	68	82	71			
Zr	195	192	99	197	190	185	177	176	178	178	204	166	179	117	92
La	78	55	57	62	68	62	54	62	54	66		63			

Table 4

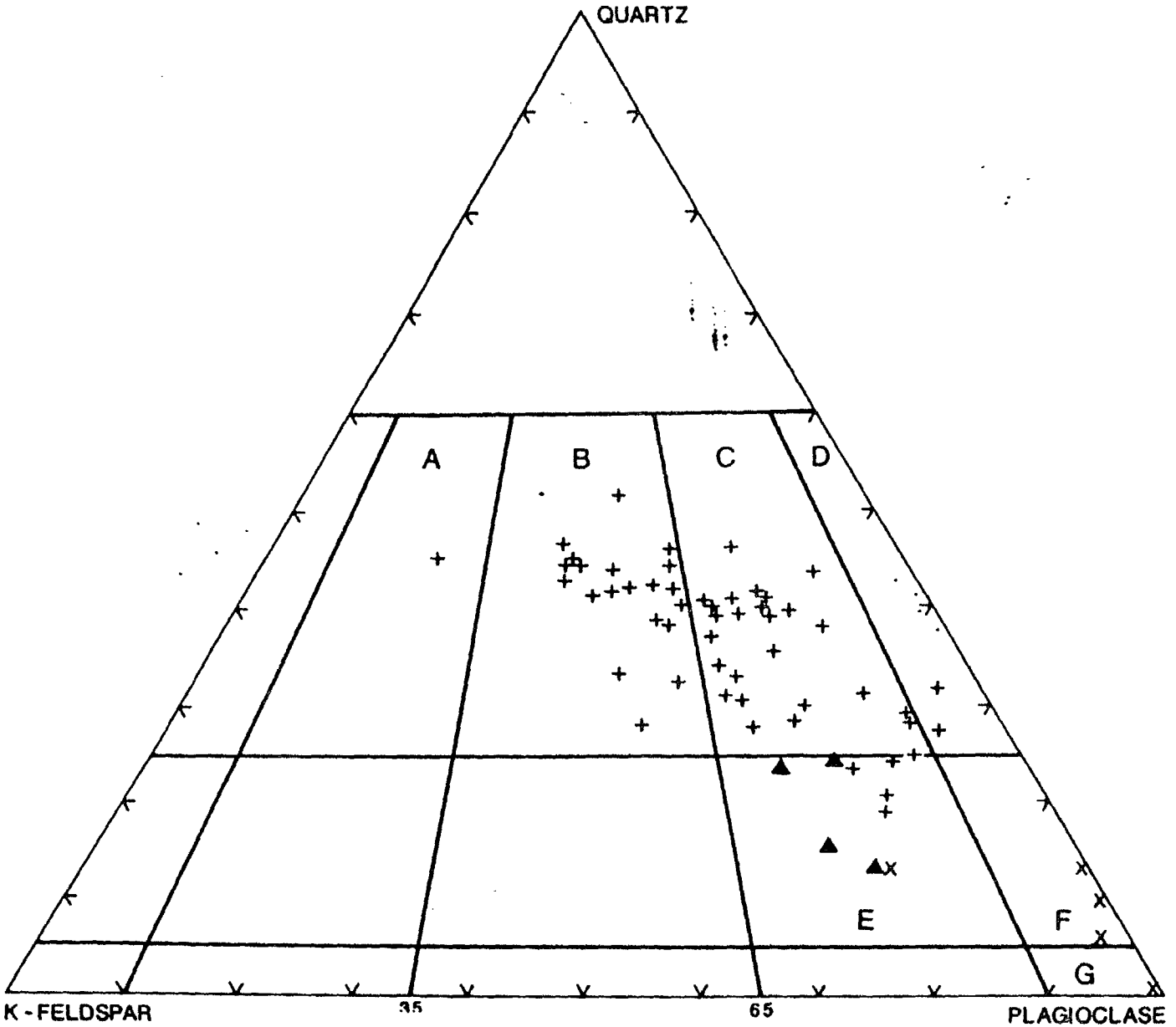

Fig 15 Modal variation of the Uralla pluton (+), Terrible Vale pluton (Δ) and Kentucky Diorite (x).

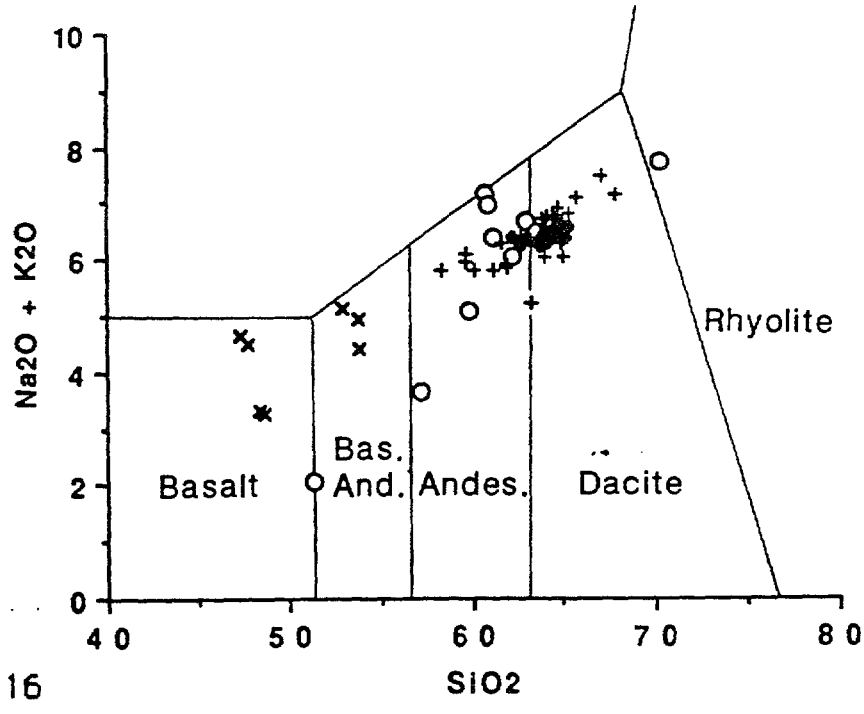

Fig 16

Analyses of the Uralla pluton (+), The Harnham Hill volcanics (o), the Terrible Vale pluton (♦) and the Kentucky Diorite (x) on a Le Bas classification diagram.

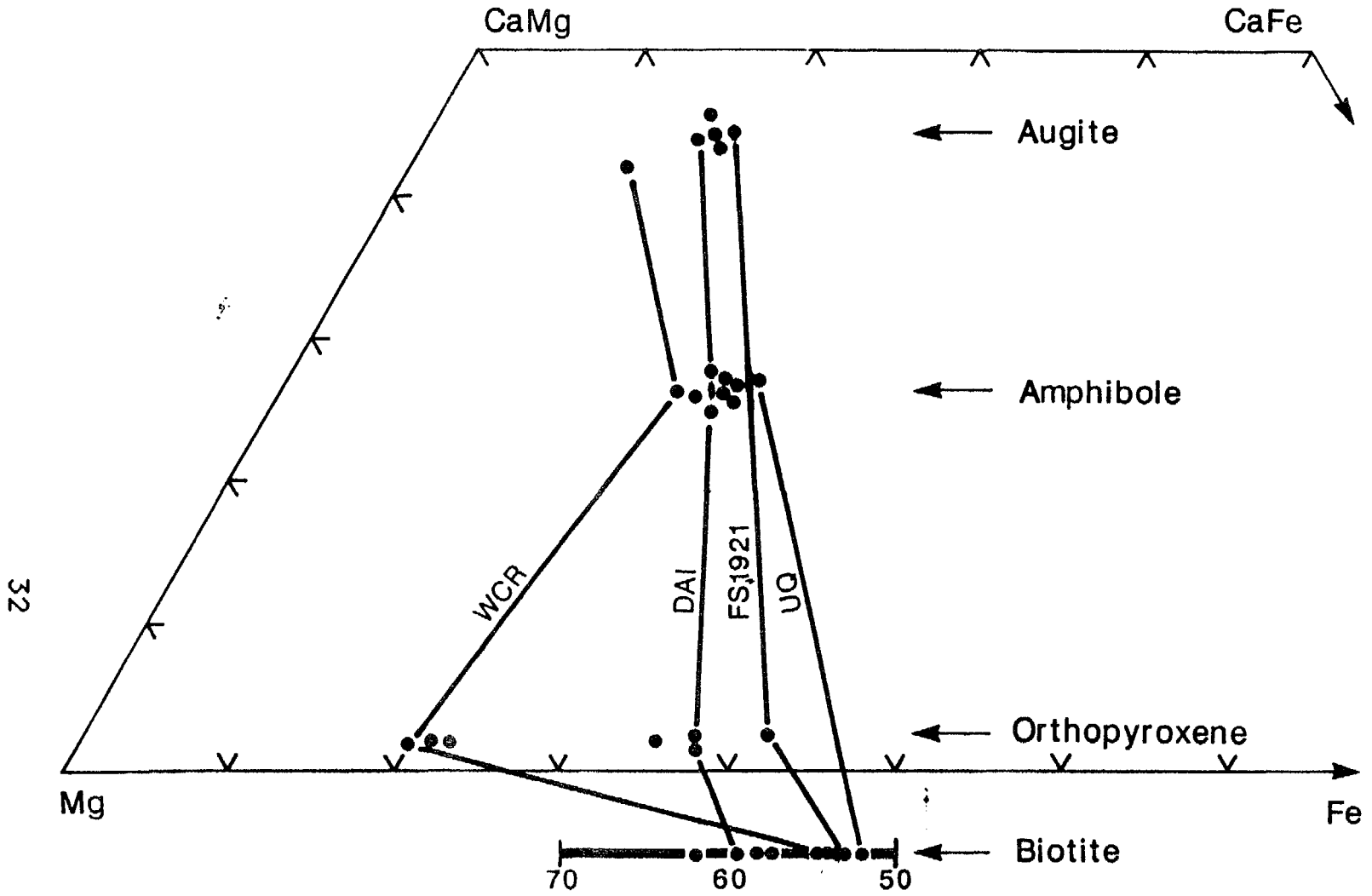

Fig 17 Compositions of the mafic minerals in the Uralla pluton (UQ), Terrible Vale pluton- chilled margin (FS1921) -centre WCR and the Kentucky Diorite (DA1).

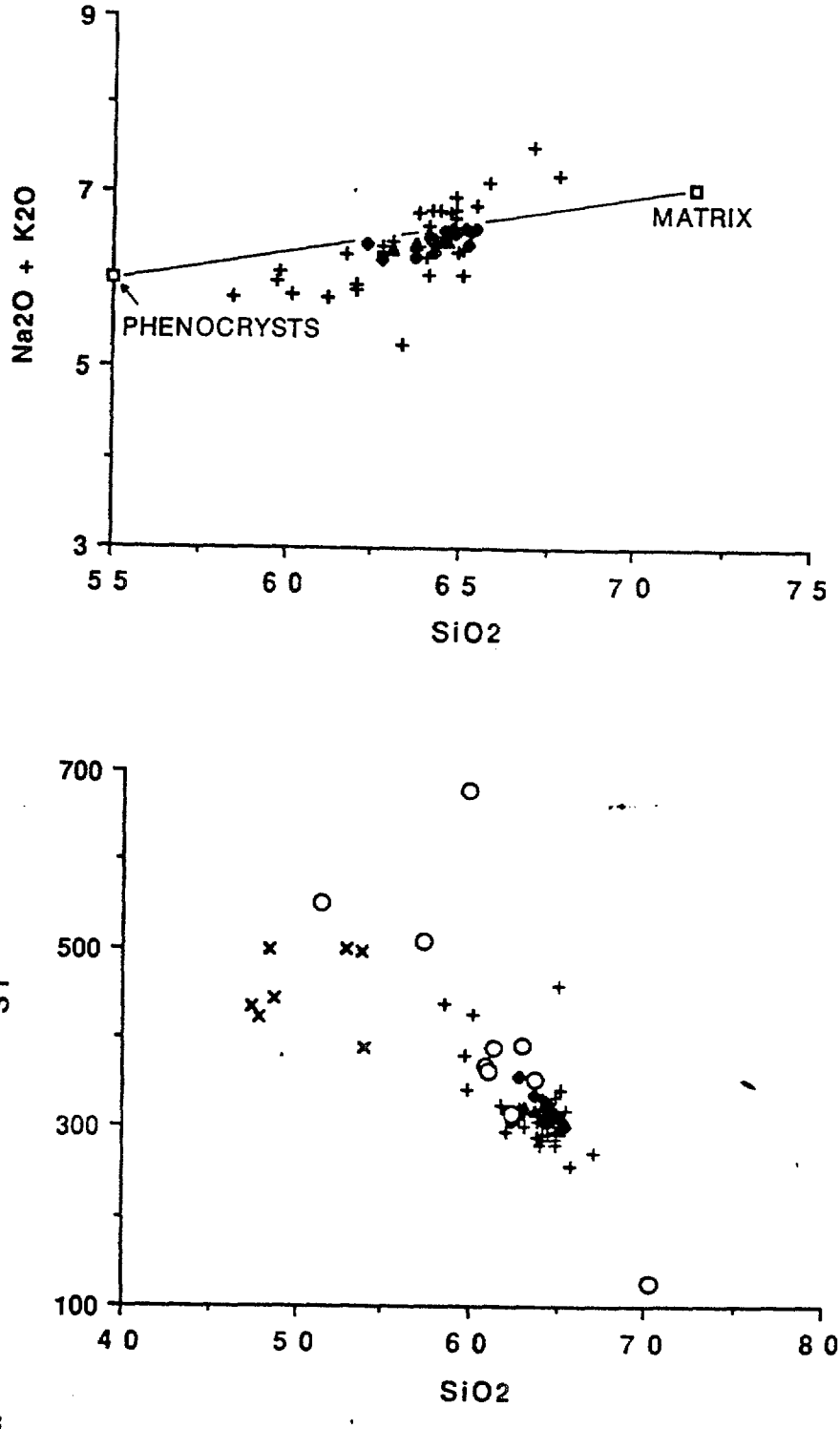

Fig 18

Plots showing the differences between the Uralla pluton (+) , Terrible Vale pluton (♦) and the Harnham Hill volcanics (o). Much of the variation in the Terrible vale pluton can be explained by fractionation involving the phenocrysts in the chilled margin (plagioclase-hypersthene-augite-ilmenite) with minor biotite. The variation in the Uralla pluton probably involves much more hornblende.

but transitional to S-type) that intrudes the sequence. In particular they are K-rich and have high normative hypersthene to diopside ratios which are also a modal characteristic of the ring dyke and the finer phases of the Terrible Vale quartz monzodiorite. Bulk rock Rb/Sr data for the Harnham Hill andesites, and facies of the Terrible Vale dacite and quartz monzodiorite, each exhibit little variation, but collectively correspond to the Uralla Pluton initial ratio of 0.7064 +/- 0.0004 based on an age of 245 Ma. Individual biotite Rb/Sr ages from rocks of the Centre range from 251-245 Ma. As with the Uralla pluton, the juxtaposition of these volcanic and sub-volcanic rocks suggests that the region has been tilted such that the highest levels are exposed in the north-east and the deepest levels in the south-west. The Terrible Vale tuffisite and quartz monzodiorite would seem to represent the uppermost parts of a magma chamber that vented to the surface during a major roof fracture event but then crystallised more slowly to produce the microstructural facies observed.

The Uralla pluton shares with the Kentucky diorite the same mineralogy and Flood and Shaw (1979) suggested that this inclusion-rich stock may be the deeper parts of the Uralla pluton not connected at the present level of erosion. The numerous dioritic inclusions, the large quartzite xenolith and the patch of biotite microgabbro all conform with the model that these rocks are formed at the bottom of the magma chamber where cumulates and stoped blocks are collecting.

The modal variation of the Terrible Vale pluton and the Uralla pluton are shown in Fig. 15. The chemical variation (Table 4) plotted on a TAS diagram is Fig 16 . Fig 17 gives a summary of the chemistry of the mafic minerals of the plutons and Fig 18 shows the difference between the variation in the Terrible Vale pluton that is inferred to result from fractionation of anhydrous minerals plus minor biotite and the variation trend of the Uralla pluton that results from fraction that involved a large component of hornblende.

FRIDAY

RETURN TO CANBERRA.

Reference:

Barnes, R. G., Brown, R. E., Brownlow, J. W. & Stroud, W. J. 1991. Late Permian volcanics in New England - the Wandsworth Volcanic Group. NSW GEOL SURV QUART NOTES **84**, 1-36.

Chappell, B. W. 1978. Granitoids from the Moonbi district, New England Batholith, eastern Australia. J GEOL SOC AUST **25**, 267-283.

Clare, A.P. 1988 Contact metamorphosed granitoids: their metamorphic zonation, correlation with associated hornfelsic isograds and implications upon emplacement mechanisms in the New England Batholith. UNPUBL.BSC. HONS THESIS MACQUARIE UNIV.

Collins, W. J. 1991. A reassessment of the 'Hunter-Bowen Orogeny': tectonic implications for the southern New England Fold Belt. AUST J EARTH SCI **38**, 409-423.

Flood, R. H. 1971. A study of part of the New England Batholith, New South Wales. PH.D. THESIS, UNIV. OF NEW ENGLAND, ARMIDALE, New South Wales, Australia.

Flood, R. H. & Shaw, S. E. 1979. K-rich cumulate diorite at the base of a tilted granodiorite pluton from the New England Batholith, Australia. J GEOL **87**, 417-425.

Flood, R. H. & Shaw, S. E. 1977. Mineralogical and chemical matching of plutonic and associated volcanic units, New England Batholith, Australia. GEOLOGY **29**, 163-170.

Hensel, H. D., McCulloch, M. T. & Chappell, B. W. 1985. The New England Batholith: constraints on its derivation from Nd and Sr isotopic studies of granitoids and country rocks. GEOCHIM ET COSMOCHIM ACTA **49**, 369-384.

Korsch, R. J. 1977. A framework for the Palaeozoic geology of the southern part of the New England geosyncline. J GEOL SOC AUST **24**, 339-355.

O'Neil, J. R., Shaw, S. E. & Flood, R. H. 1977. Oxygen and hydrogen isotope compositions as indicators of granite genesis in the New England Batholith, Australia. CONTRIB MINERAL PETROL **62**, 313-328.

Ransley, J. R. 1970 The petrology of the New England Batholith: Yarrowyck-Balala-Uralla area, north-eastern N.S.W. UNPUBL. MSC THESIS UNIV NEW ENGLAND.

Shaw, S. E. & Flood, R. H. 1981. The New England Batholith, eastern Australia: geochemical variations in time and space. J GEOPHYS RES **86**, 10530-10544.

Teale, G.S. 1974. Thermal metamorphic schists adjacent to the Walcha Road Adamellite, New England , New South Wales. UNPUBL. BA HONS THESIS MACQUARIE UNIV.

Thompson, S. 1988 The Balala Yarrowyck dyke swarm: some petrological and structural aspects. UNPUBL BSC HONS MACQUARIE UNIV.

Vernon, R. H., Flood, R. H. & D'Arcy, W. F. 1987. Sillimanite and andalusite produced by base-cation leaching and contact metamorphism of felsic igneous rocks. J METAMORPHIC GEOL **5**, 439-450.